

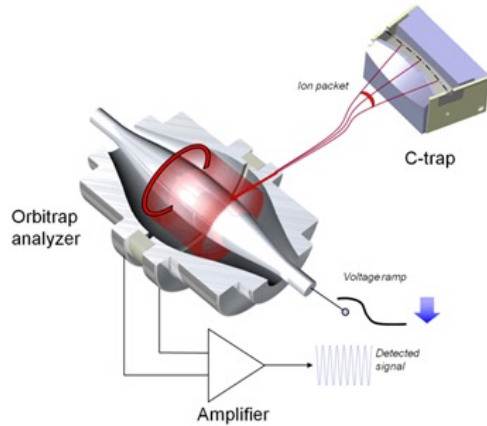
Emission Characteristics of a Broad-Area Molybdenum Cathode under Inhomogeneous Electric Field

Moein Borghei, Robin Langtry

03/04/2024

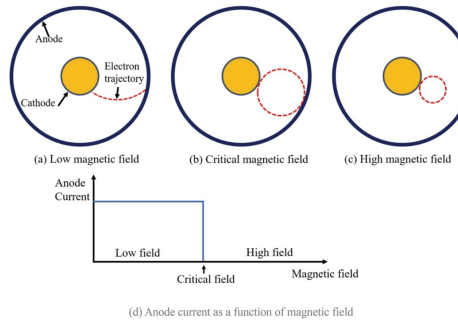


Orbitrap



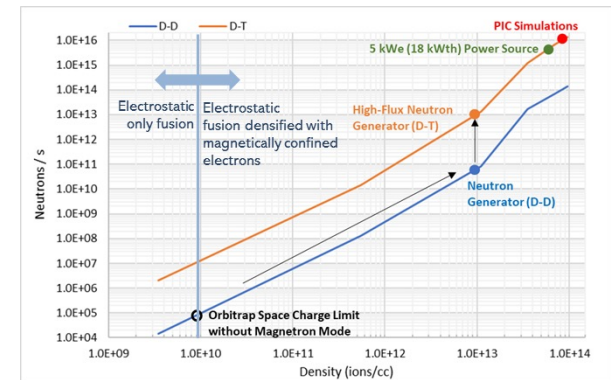
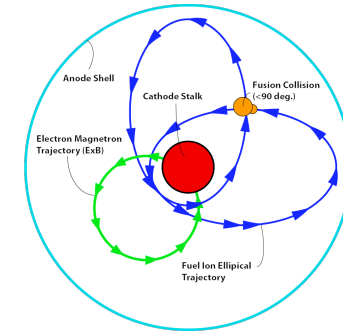
- Ion beam confined electrostatically in orbits around spindle shaped cathode and outer anode shell

Magnetron



- Electrons confined in ExB field between cathode and anode
- Long electron confinement times and low current between cathode and anode

Orbitron



- Dense high energy plasmas
- Bright neutron sources via D-D and D-T fusion
- Potential for small net energy fusion devices

Electrostatic & Non-Thermal Fusion Plasma

Electrostatic & Non-thermal (non-Maxwellian) fusion plasma is controversial in fusion sciences

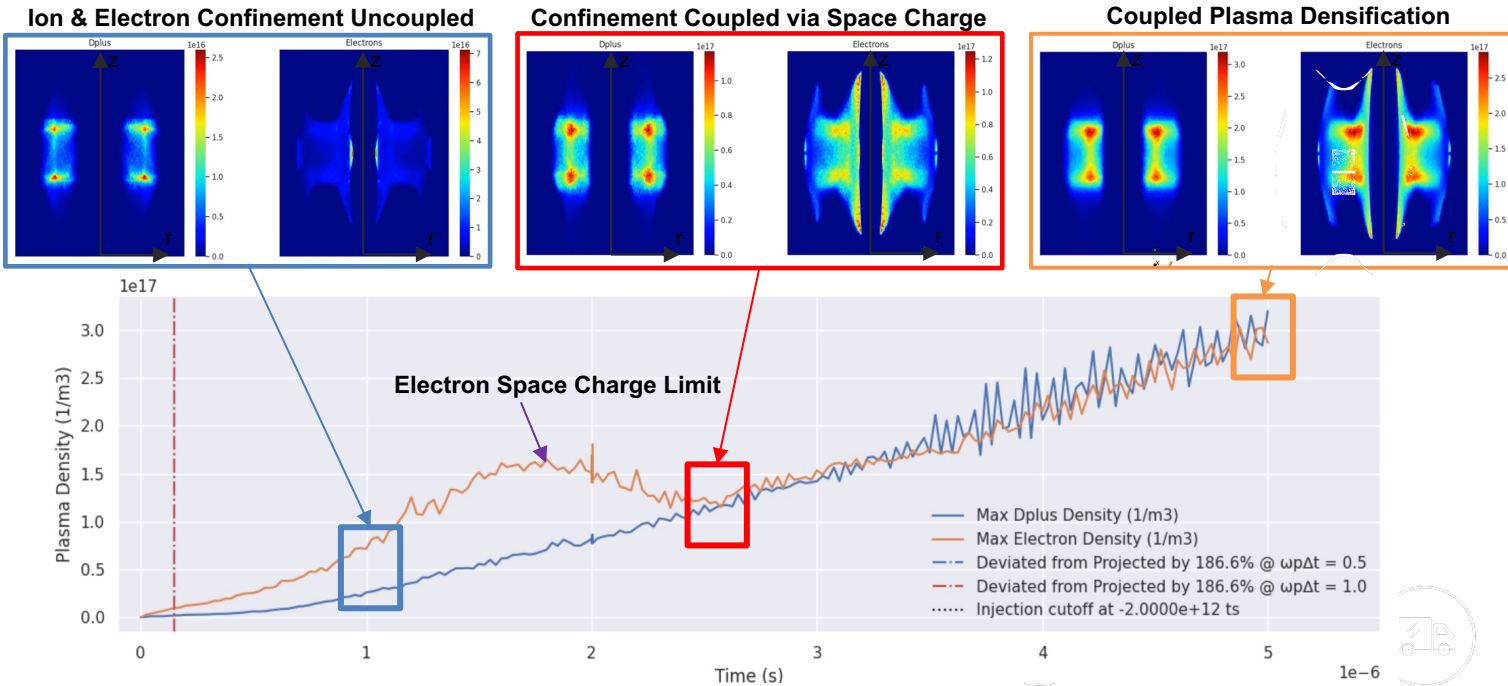
At a high level for D-T plasma the scientific critics (e.g. Rider 1995, Lampe & Manheimer 1998) can be summarized as two key points:

- A) Electrostatic approaches to fusion cannot achieve high ion densities due to space charge effects
- B) Electrostatic or Non-thermal (Non-Maxwellian, colliding beam) approaches to fusion cannot achieve net energy due to excessive Coulomb collision losses

Space Charge Density

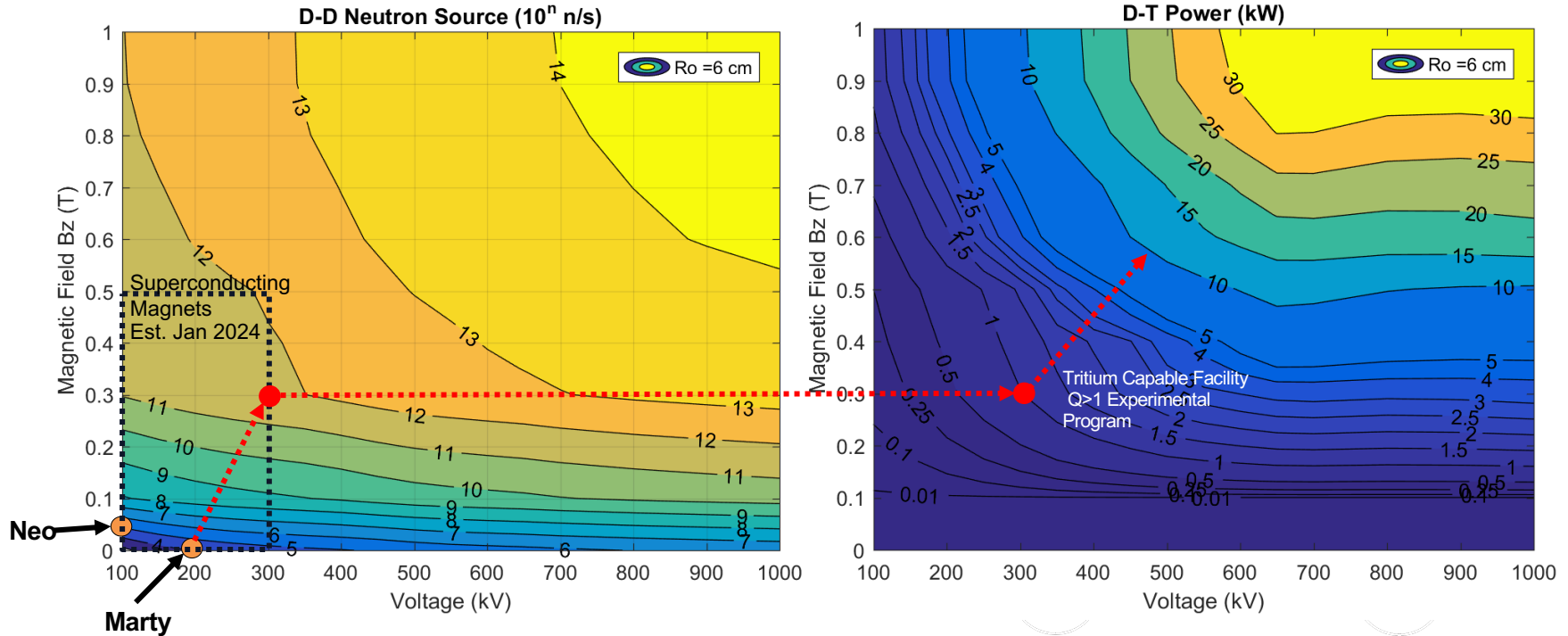
- In Orbitron electrons are introduced and confined via magnetron ExB electron scheme to overcome ion space charge density limits

PIC Simulations showing ion and electron loading into the Orbitron, exceeding space charge limit and ultimately densified plasma

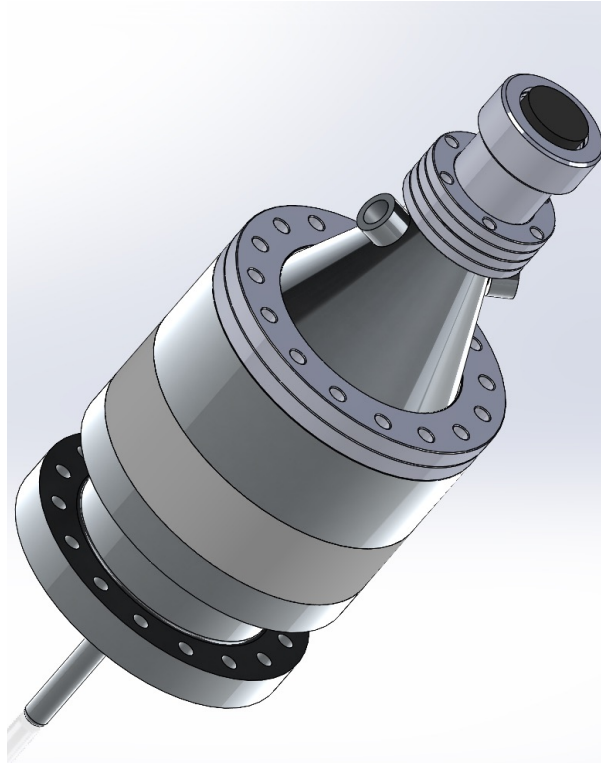


Orbitron Experimental Program Current Status

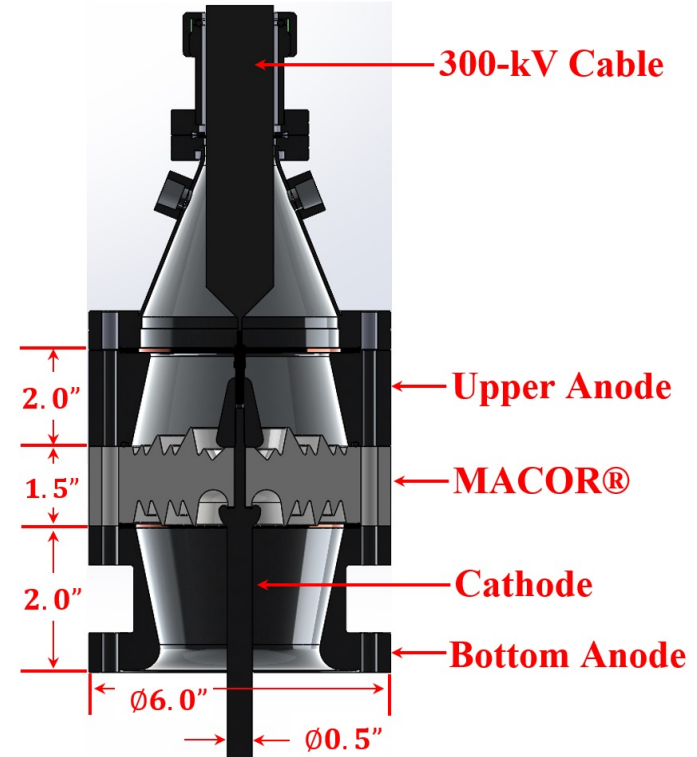
- Prototype 1 (Neo): Measured fusion neutrons at 100 kV, 0 T (no magnets): 1E4 n/s
- Prototype 1 (Neo) : Working on Improved ion loading + magnets 100 kV, 0.05 T: $\approx 1E6$ n/s
- Prototype 2 (Marty): Reached 200kV (no magnets) and Targeting 300 kV, 0.3 T in 2024: $\approx 1E11$ n/s



- Avalanche's first bushing design



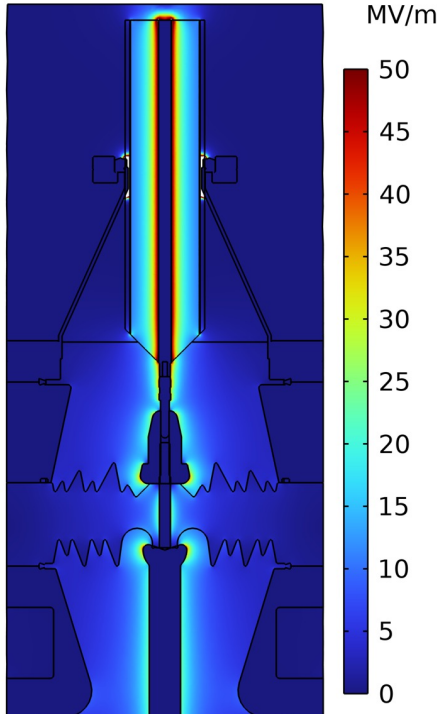
3D model of MAKO[®] in SOLIDWORKS[®]



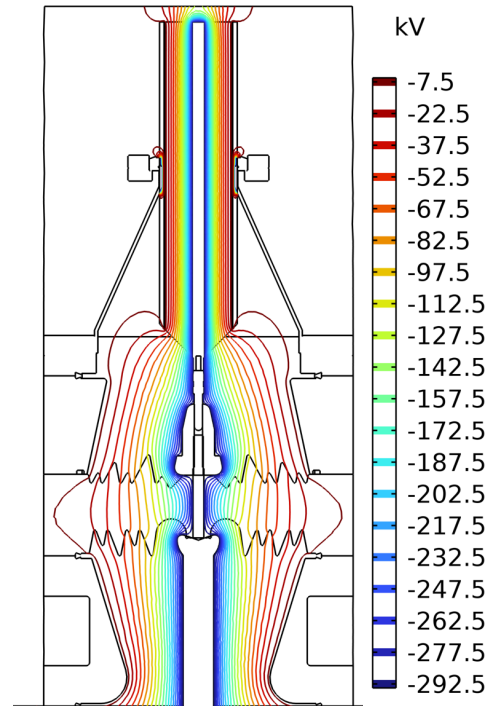
Cross-section of MAKO[®] model in SOLIDWORKS[®]

M. Borghei, et al, "A Compact, 300-kVDC Bushing for Operation under Ultra-High Vacuum Pressure," 2022 IEEE Conference on Electrical Insulation and Dielectric Phenomena (CEIDP), Denver, CO, USA, 2022, pp. 471-474, doi: 10.1109/CEIDP55452.2022.9985264.

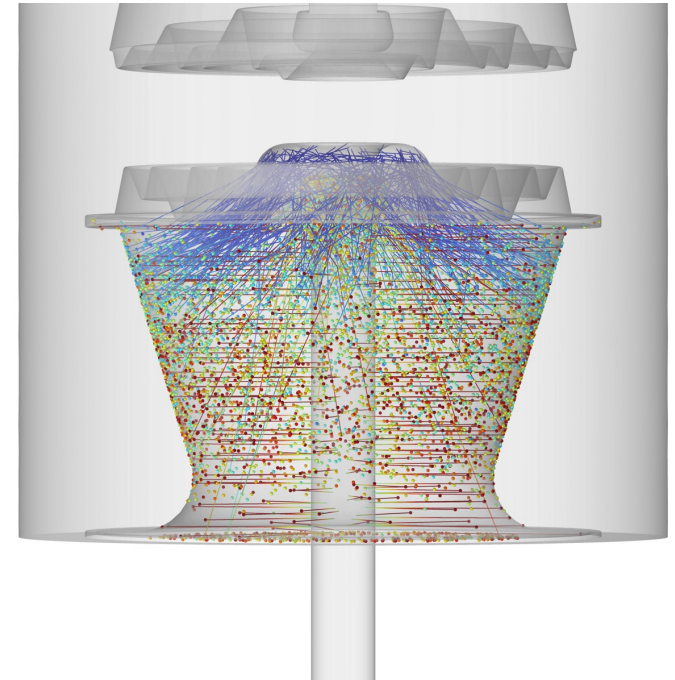
- Voltage contours and electric field distribution simulated in COMSOL Multiphysics®



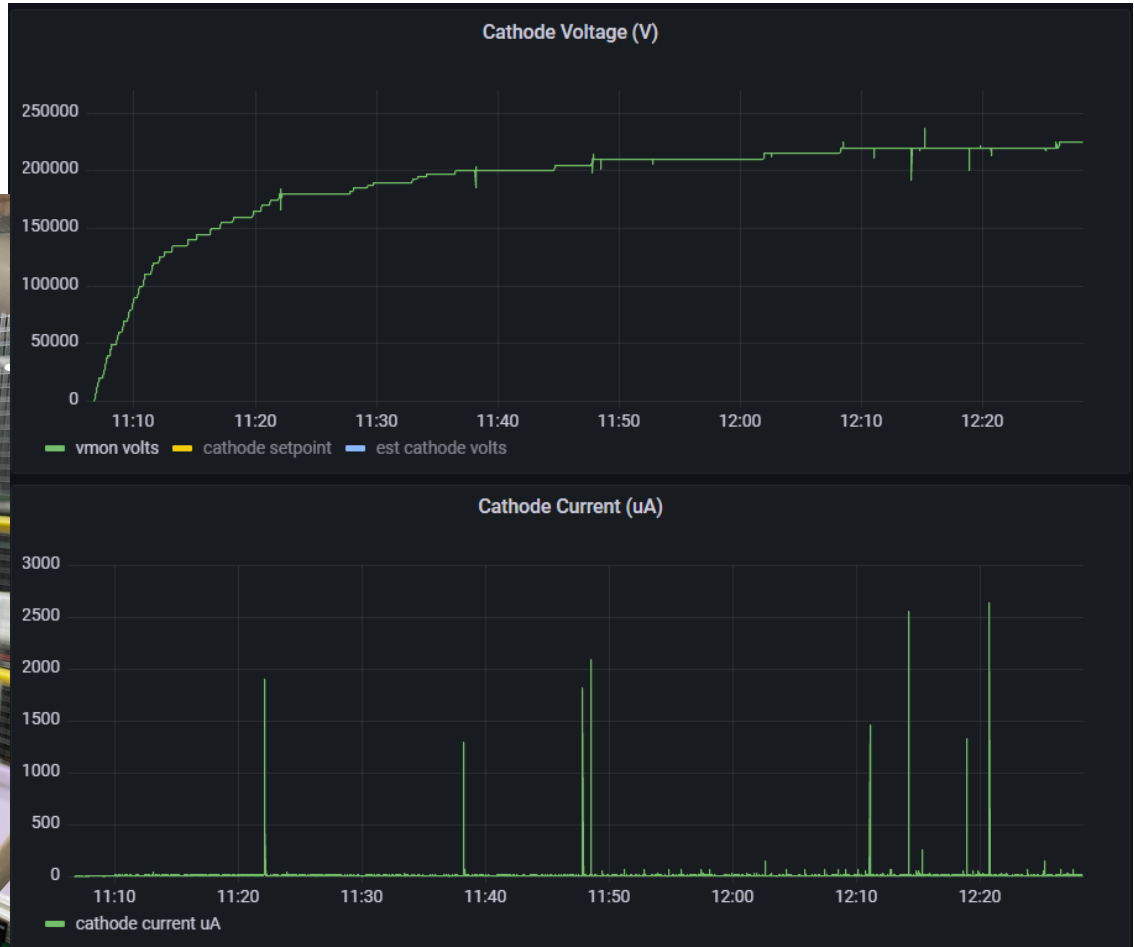
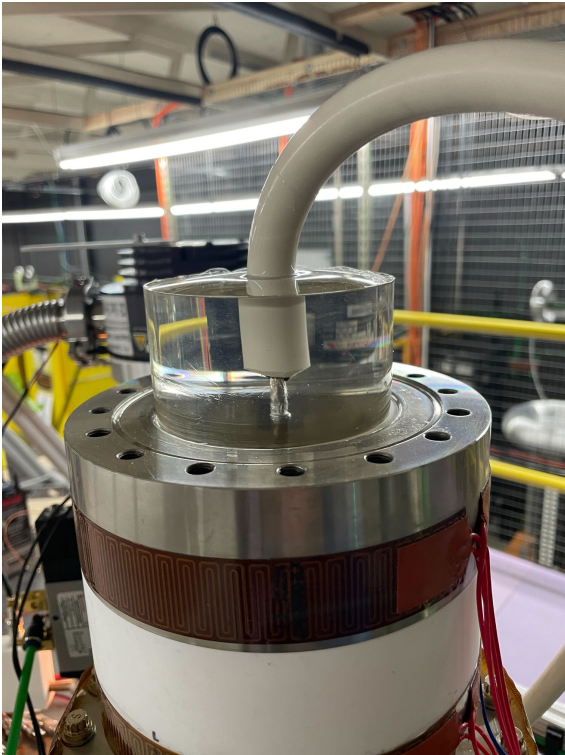
Electric field distribution in the cross-section of MAKO®.



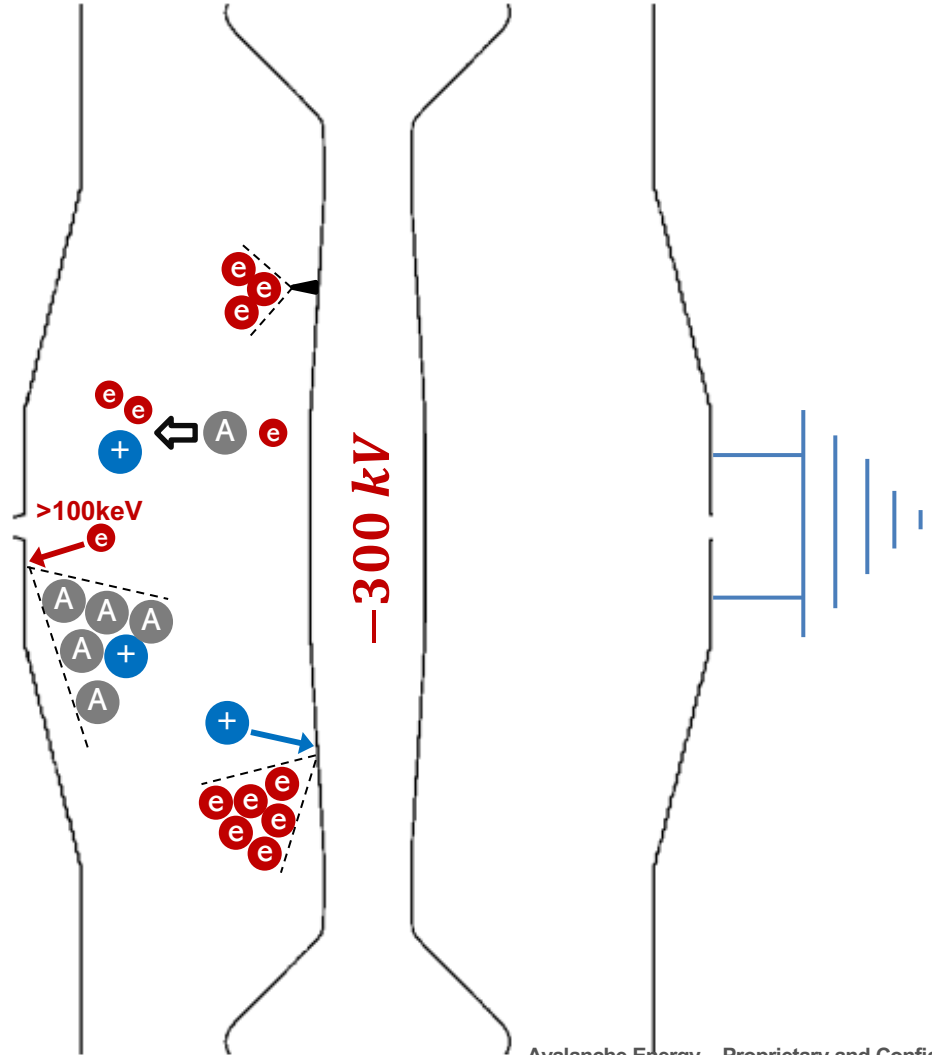
Voltage distribution in the cross-section of MAKO®.

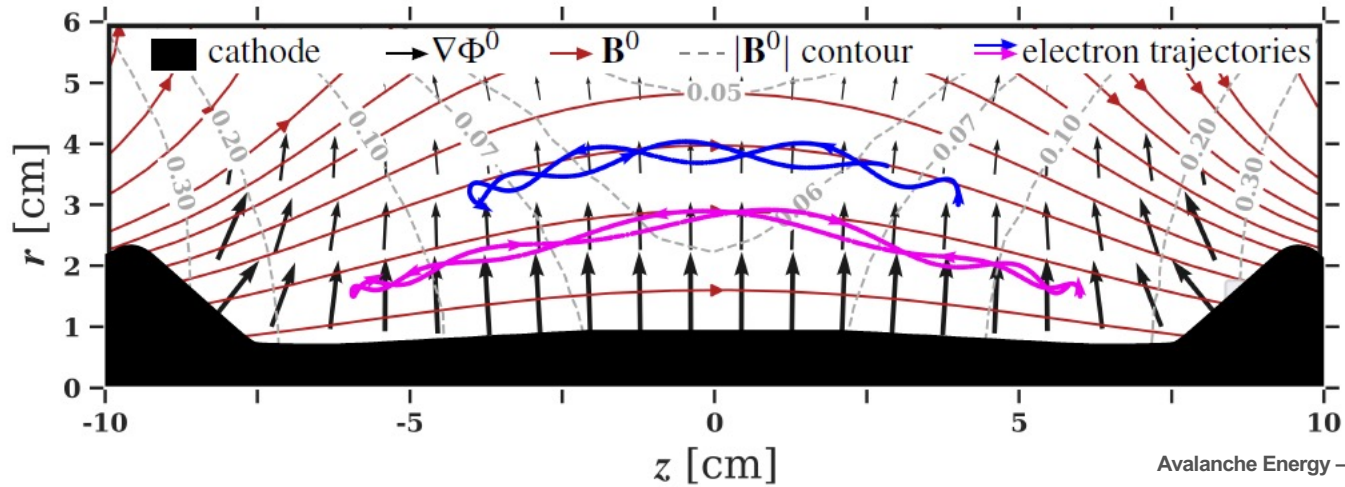
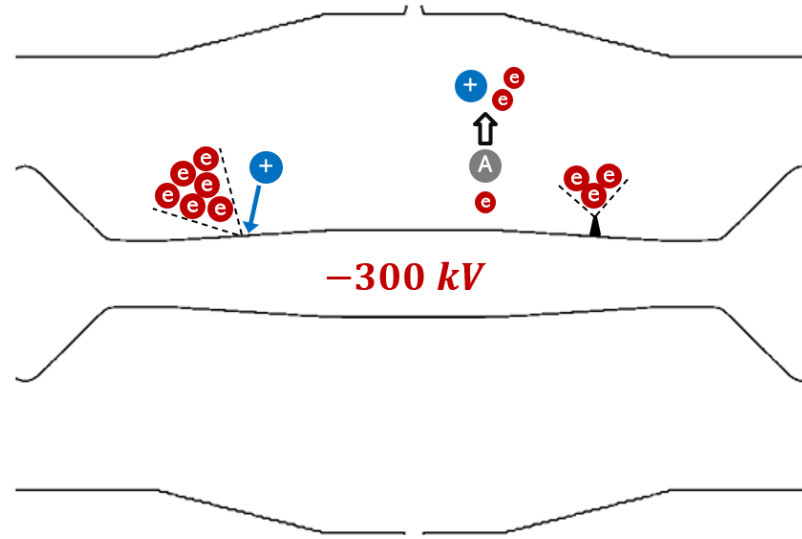


- Voltage and current measurements during the HV conditioning



- Field Emission of Electrons
- Electron impact ionization
- Gas desorption from anode
- Ion-induced secondary electron emission from cathode





- An input to the simulation models is the electron source off of the Collective emission model

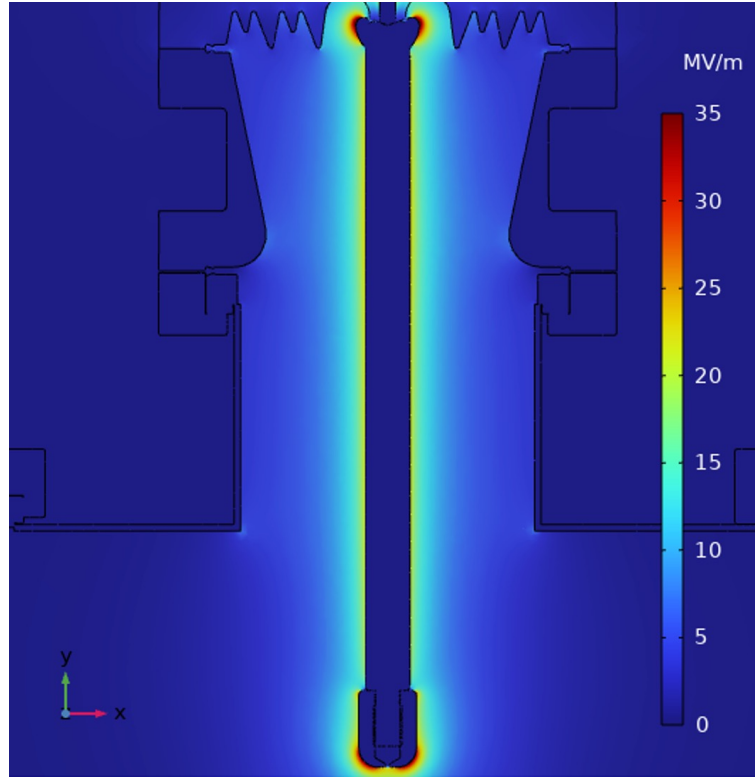
$$J = C_1 \frac{(\beta E)^2}{\phi t(y)} \exp\left(-\frac{C_2 \phi^{\frac{3}{2}} v(y)}{\beta E}\right)$$

$$I = \sum_{i=1}^N A_i C_1 \frac{(\beta_i E_i)^2}{\phi_i} \exp\left(-\frac{C_2 \phi_i^{\frac{3}{2}}}{\beta_i E_i}\right)$$

$$I = \sum_{i=1}^N A_i C_1 \frac{(\beta_i E_i)^2}{\phi_i} \exp\left(-\frac{C_2 \phi_i^{\frac{3}{2}}}{\beta_i E_i}\right)$$

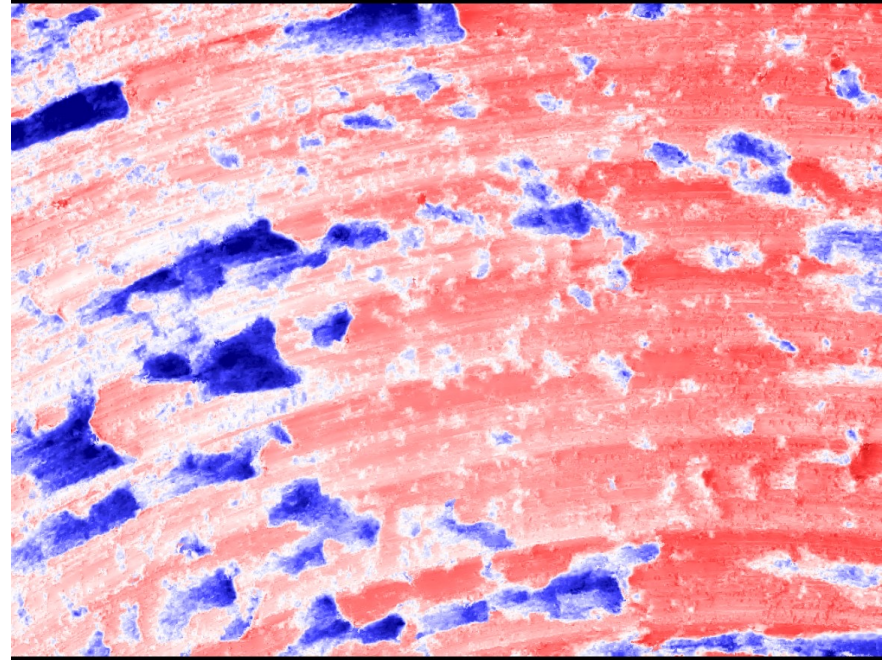
Informed by LIBS (green arrow pointing to N)
 Informed by LIBS (red arrow pointing to A_i)
 Informed by AES (blue arrow pointing to ϕ_i)
 ? (yellow arrow pointing to C_2)
 Informed by Electrostatic Simulation (purple arrow pointing to $\beta_i E_i$)

(1) Macroscopic electric field at the surface of cathode

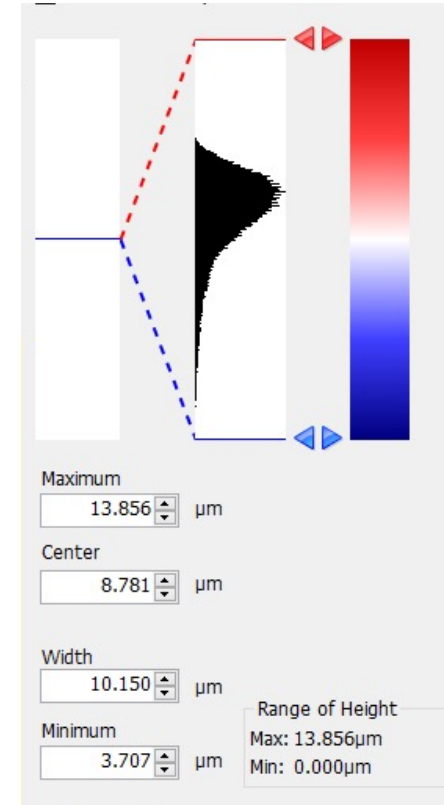
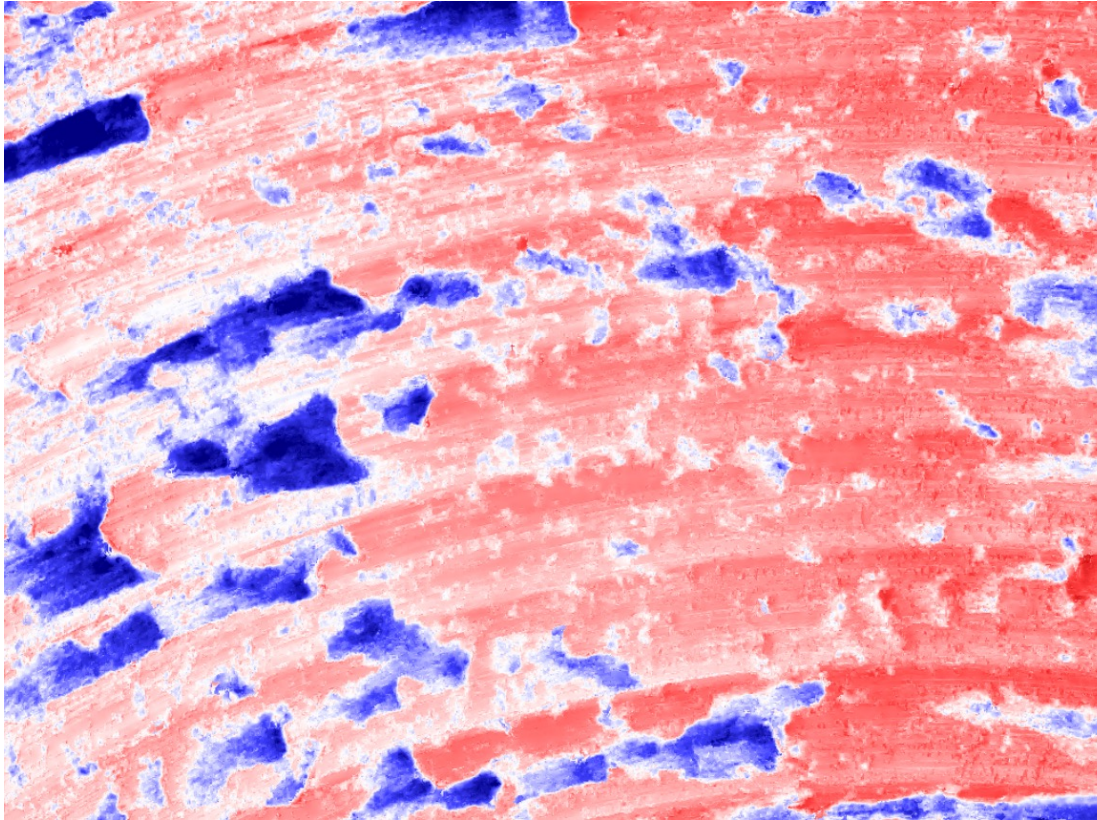


(2) Emission sites' population and geometry

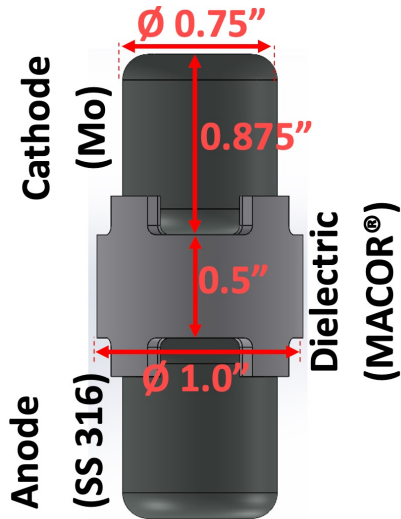
- Laser-induced breakdown spectroscopy:



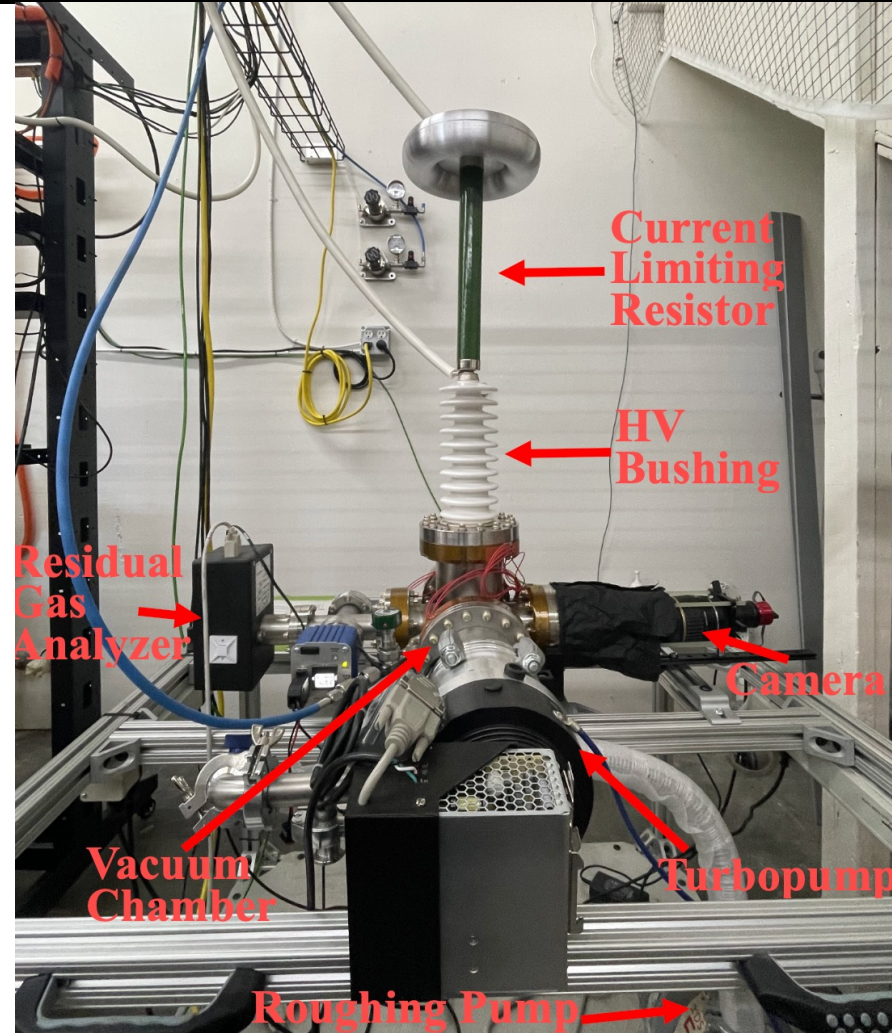
- LIBS surface roughness



(3) Surface Constituents

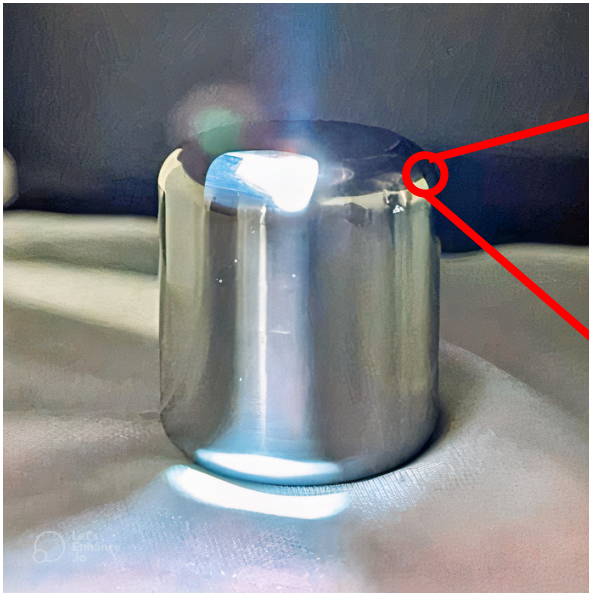


The assembly of test samples.

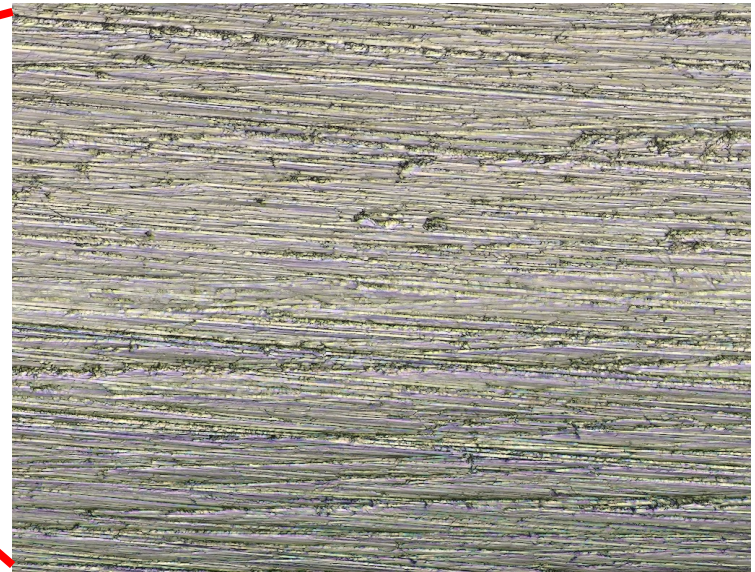


High voltage test setup

- Optical imaging of the Mo samples with a 3D reconstruction from the laser profile.

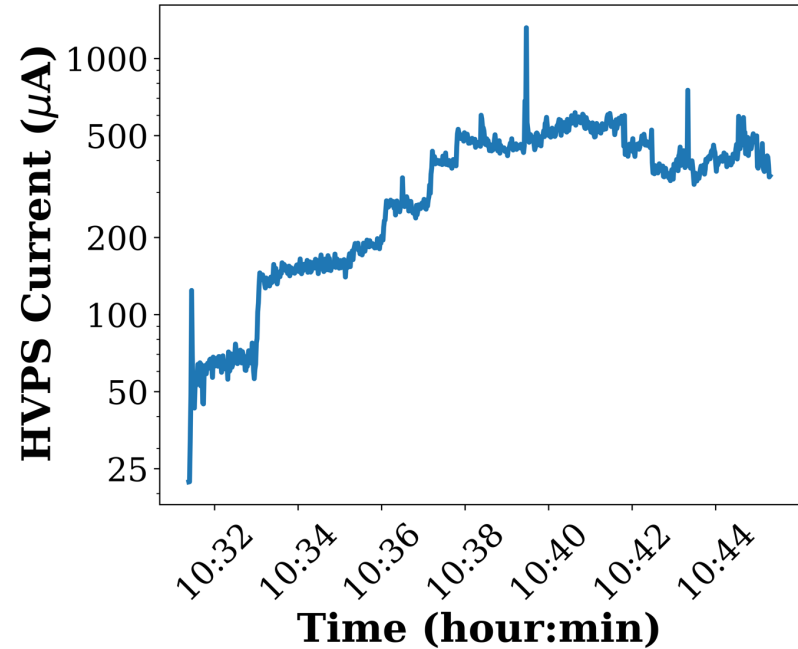
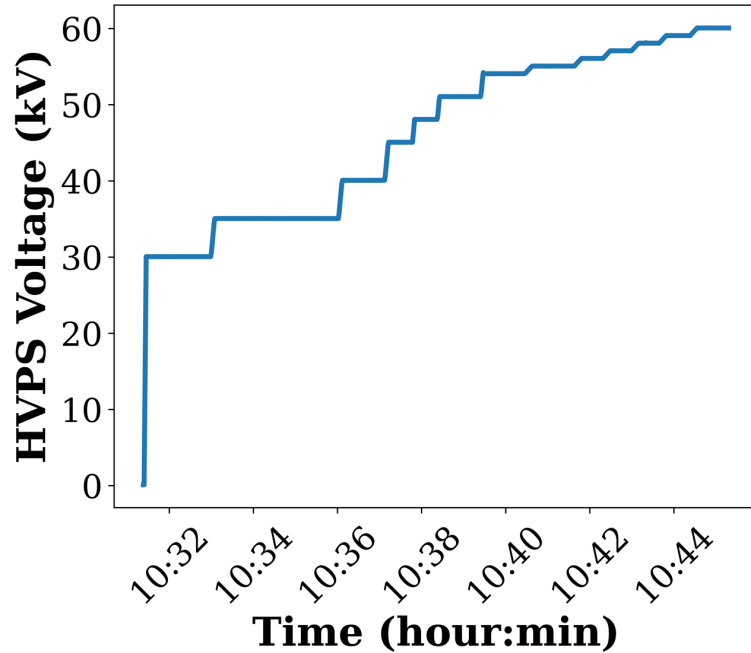


The molybdenum sample.



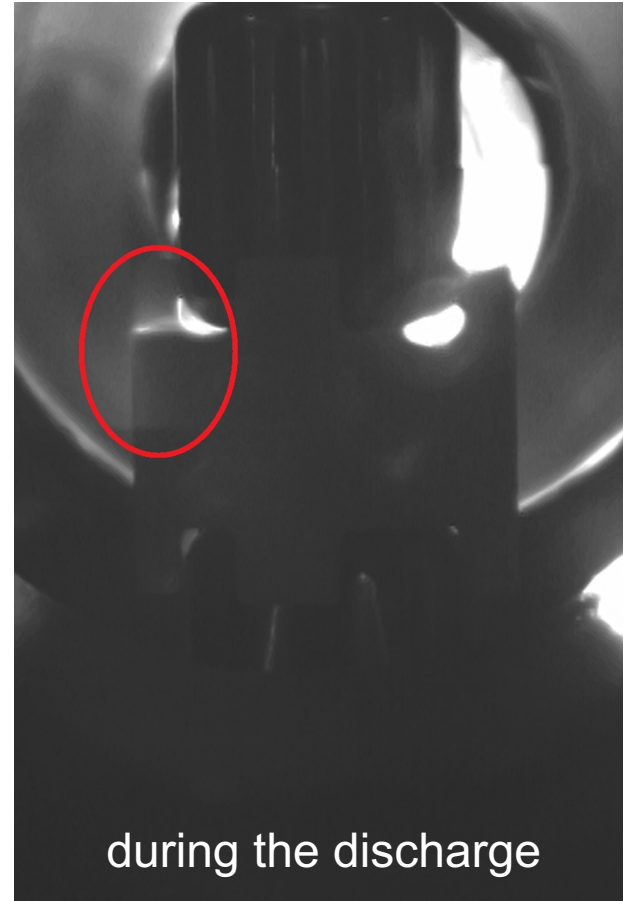
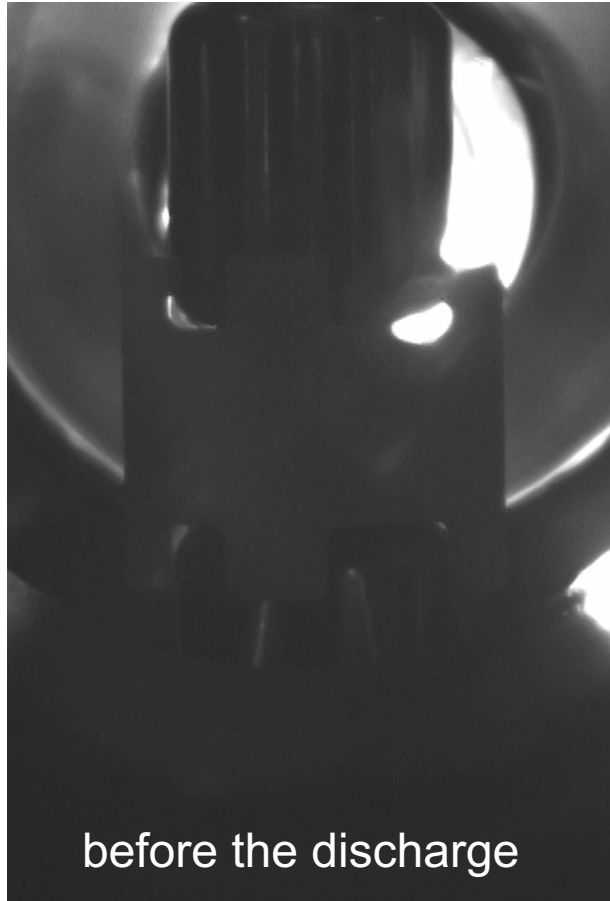
50x-magnified optical image

- First Test Campaign: *Characterization of Chemical Impact of Conditioning*

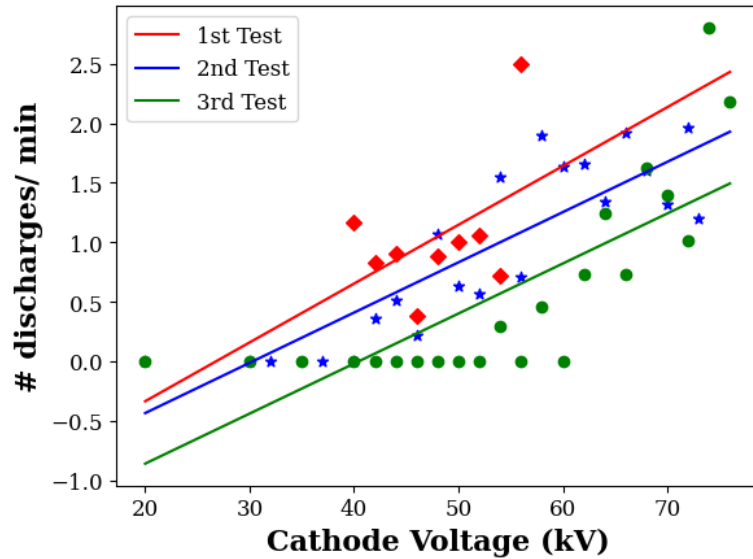


M. Borghei, et al, "Impact of Direct Current Conditioning on Cathode Dark Current in High Vacuum," 2023 30th International Symposium on Discharges and Electrical Insulation in Vacuum (ISDEIV), Okinawa, Japan, 2023, pp. 74-77.

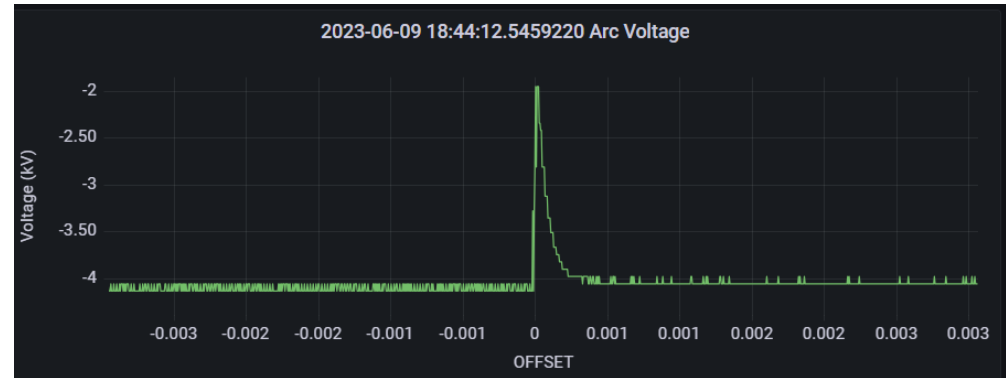
Camera capturing the side view of the samples



Evolution of Performance over Time



Test	Initial Pressure	Max Voltage	V_{min} with 10 discharges	#discharges at 56 kV	Dark current at 56 kV
1	26 nTorr	56 kV	56 kV	10	34 μA
2	10 nTorr	73 kV	58 kV	2	34 μA
3	13 nTorr	76.1 kV	74 kV	1	36 μA

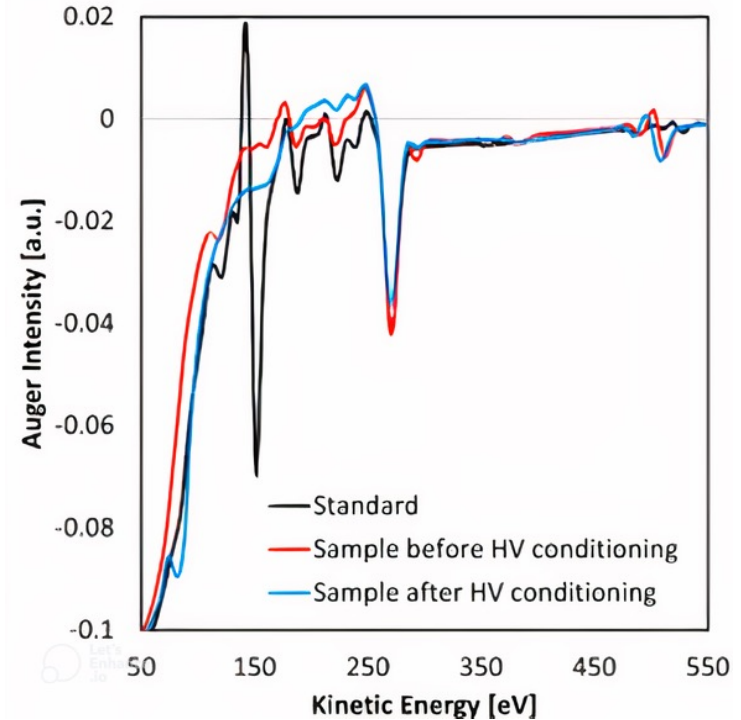


M. Borghei, et al, "The Aging Effect of Surface Flashovers on Insulator Surface in Vacuum: A Case Study," 2023 IEEE Conference on Electrical Insulation and Dielectric Phenomena (CEIDP), East Rutherford, NJ, USA, 2023, pp. 1-6, doi: 10.1109/CEIDP51414.2023.10410573.

- Average surface roughness before and after HV conditioning quite similar ($1.87 \pm 0.41 \mu\text{m}$ and $1.96 \pm 0.36 \mu\text{m}$, respectively.)
- No significant impact on surface morphology

Relative Atomic Percentual Concentrations from AES Spectra

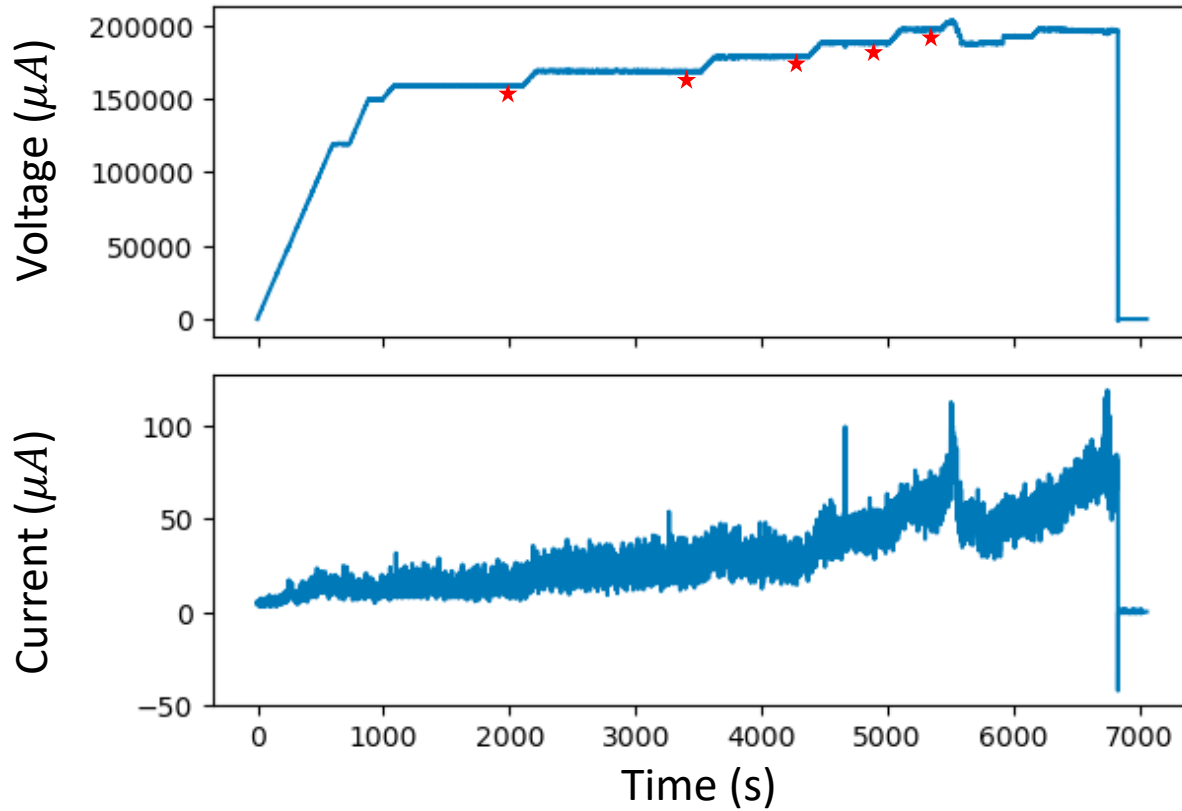
Sample	Standard	Before Conditioning	After Conditioning
C	19.59	21.72	33.98
O	2.10	1.59	14.15
Mo	78.31	0.65	1.42
W	-	74.73	49.78
Si	-	0.57	0.35
Ca	-	0.74	0.33



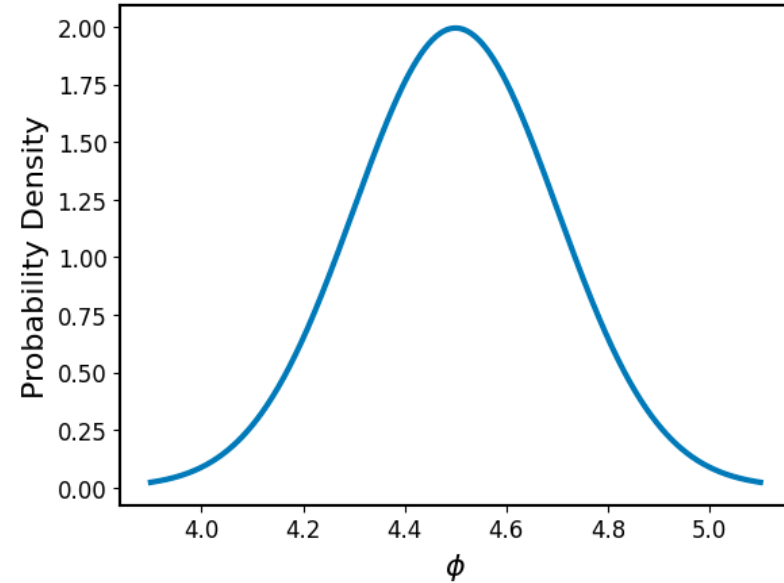
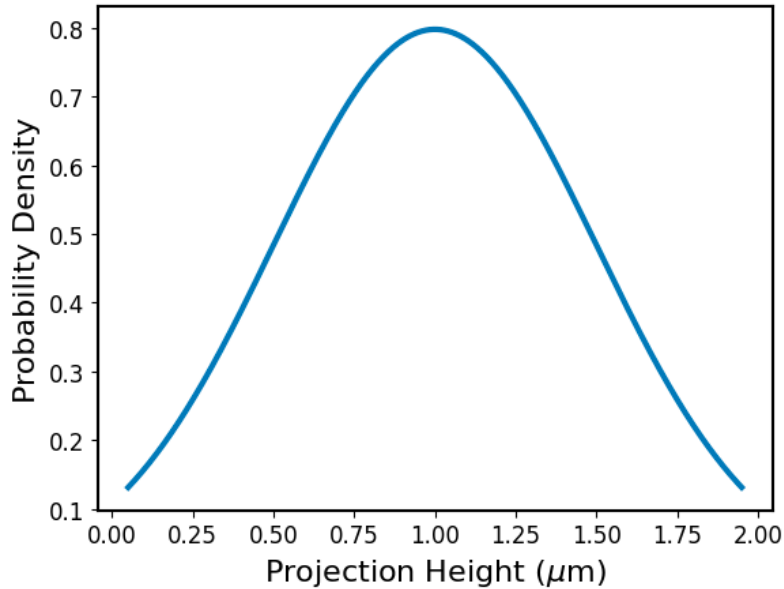
Auger electron spectra of Mo sample.

M. Borghei, et al, "Impact of Direct Current Conditioning on Cathode Dark Current in High Vacuum," 2023 30th International Symposium on Discharges and Electrical Insulation in Vacuum (ISDEIV), Okinawa, Japan, 2023, pp. 74-77.

- Test data at the conditioned points

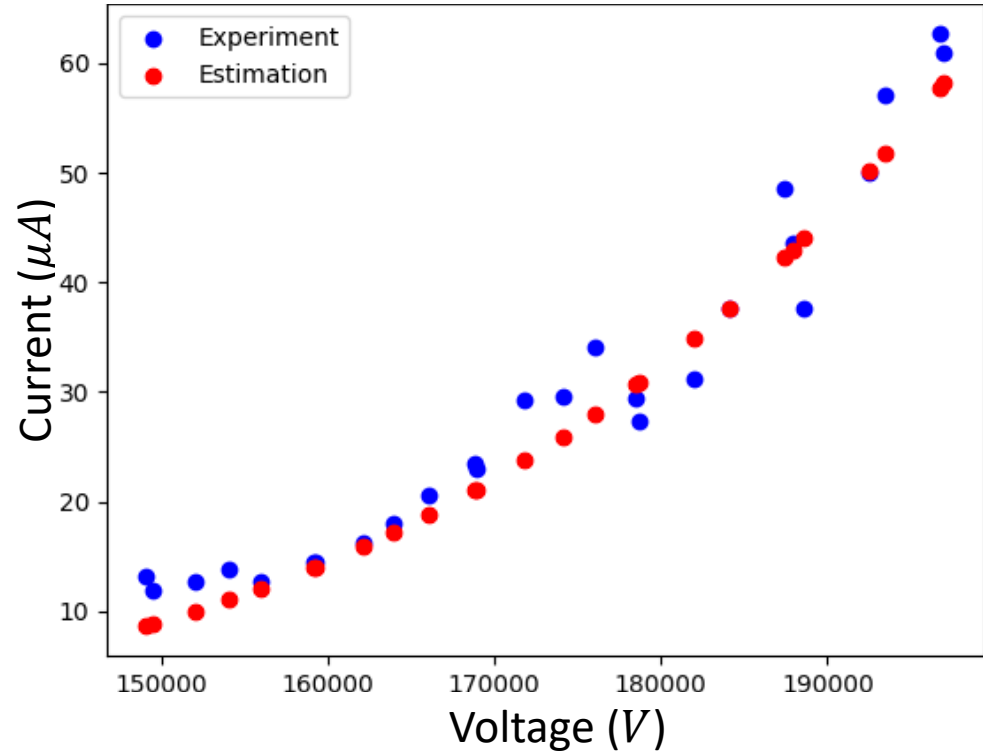
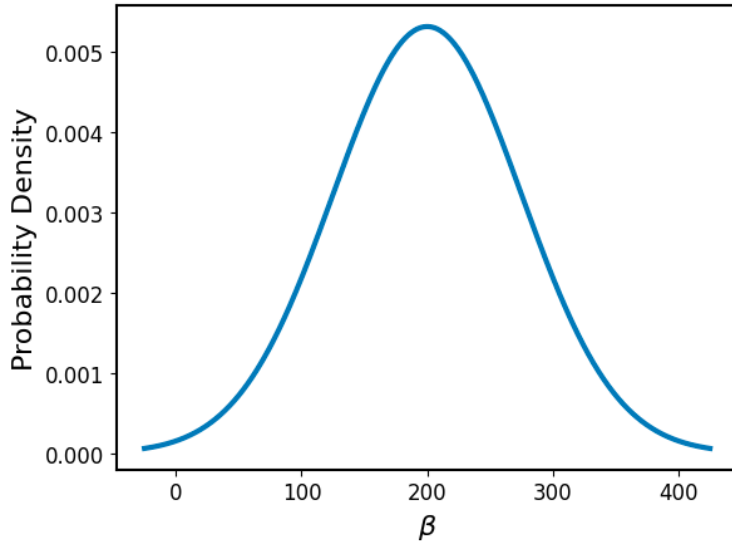


- Assumptions for the probability distributions of work function and projection height



$$A = 2\pi \left(\frac{H}{\beta - 2} \right)^2$$

- Number of Sites = 350
- Mean Square Error = $1.181042e-11$



Summary

- Electron emission current from the cathode → an important input to the PIC simulations
- Multiple broad area sections of cathode need a collective model of field emission
- An informed model was built using
 - (1) Macroscopic electric field data
 - (2) AES for finding the surface constituents
 - (3) LIBS for the scale of micro-protrusions
- An optimized collective electron emission based on FE site population and β probability distribution
- Future work to incorporate a larger dataset and also include the ion-induced SEE

Thank you.

mborghei@avalanche.energy

Actively hiring and looking forward to
collaborations





AVALANCHE

Electrostatic Non-Thermal Fusion Plasma

Much of the previous controversy stems from the modelling assumptions in the reduced order models used to assess the various fusion concepts ... the real fusion and confinement physics are complicated!

We find the two high-level critics: Space Charge and Coulomb Collisions are valid

BUT the Orbitron also has some unique aspects that address both issues

First-order models to understand the high-level Orbitron physics



Particle-in-Cell simulations to incorporate the complex physics



Experimental prototypes to anchor the first-order models and simulations

Coulomb Scattering Collisions: 2.5D PIC Simulation

Using PIC Simulation with LBNL's WarpX code to anchor and validate conclusions from first-order model

WarpX includes state-of-art relativistic Coulomb collision models and fusion reactions

Some Caveats:

Time step is set by electrons at $5E-13$ s

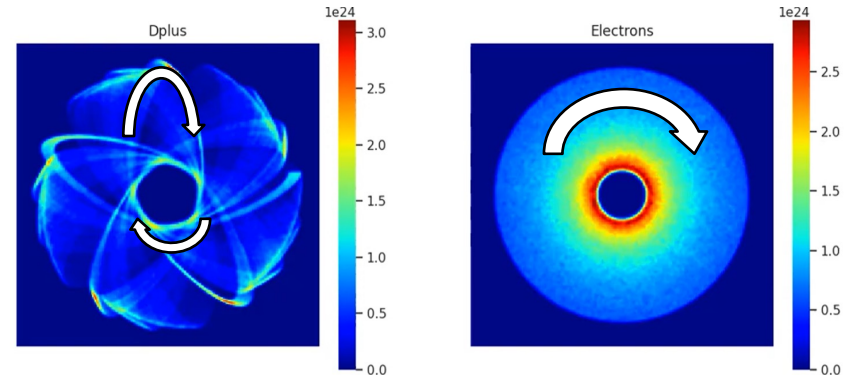
At a target Orbitron density of $5E19/m^3$ estimated complete thermalization time from Lampe & Manheimer for D-T plasma is 0.05 seconds

To make computationally tractable simulation is run at densities from $1E25/m^3 - 5E23/m^3$

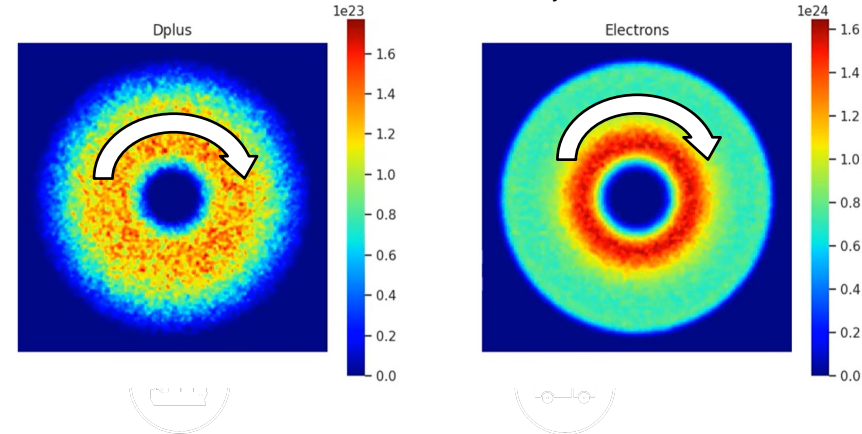
Not possible to resolve plasma frequency or space charge at these densities, simulation is purely a Monte-Carlo Coulomb scattering test case

Results are density scaled back to Orbitron densities of $5E19/m^3$

PIC Simulations initial ion and electron density distribution axial view



PIC Simulations thermalized ion and electron density distribution axial view



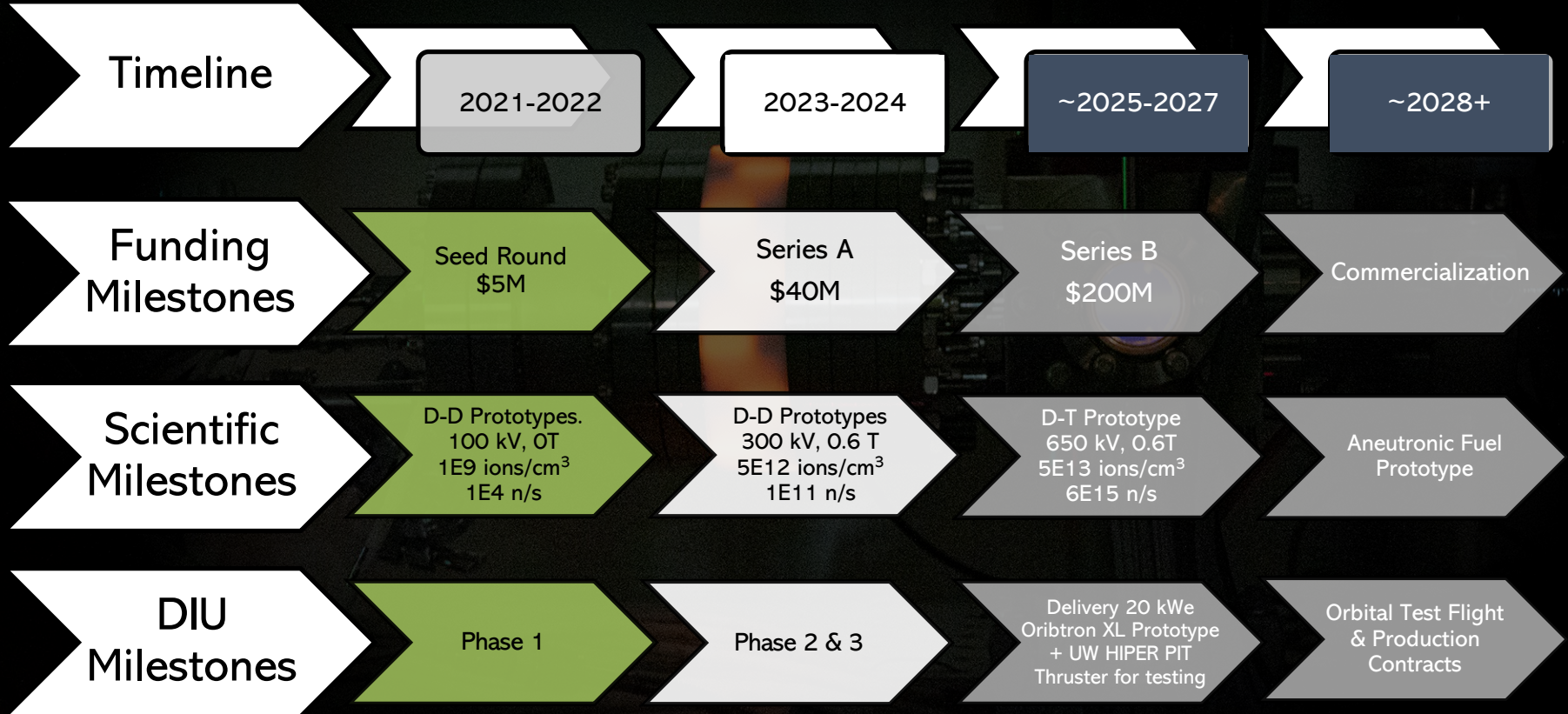
Material Characterization

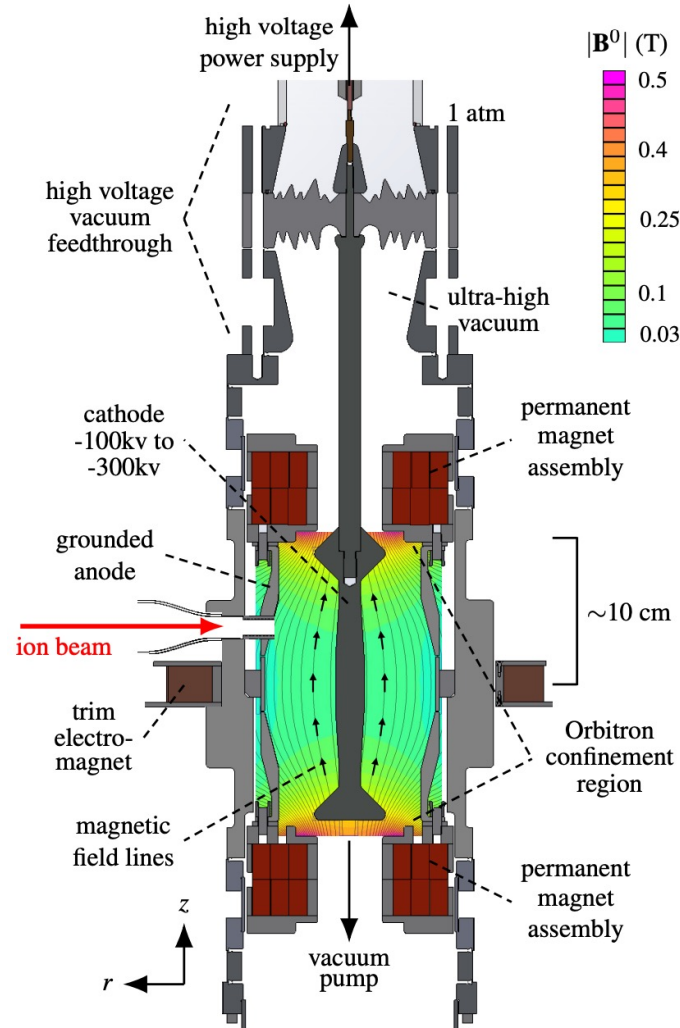
Dielectric	MACOR	Alumina	Alumina	Zirconia	Zirconia	BN	Shapal	Quartz (Fused Silica)	AlN	Mullite
Grade	-	99.9%	99.6%	TTZ-C	ZTA	Grade A	-	-	-	-

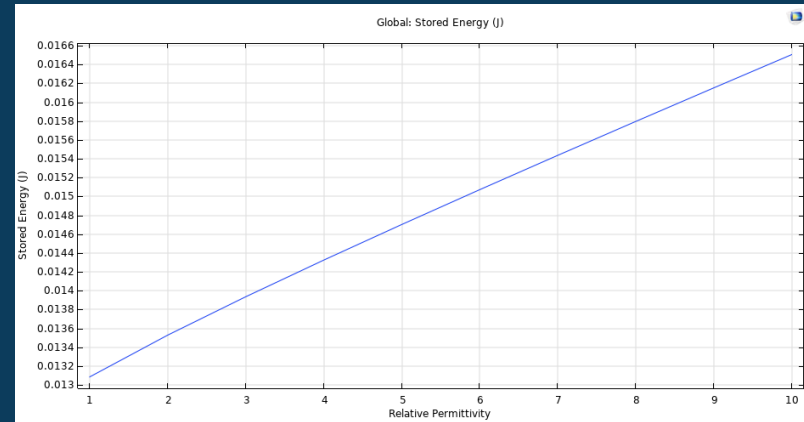
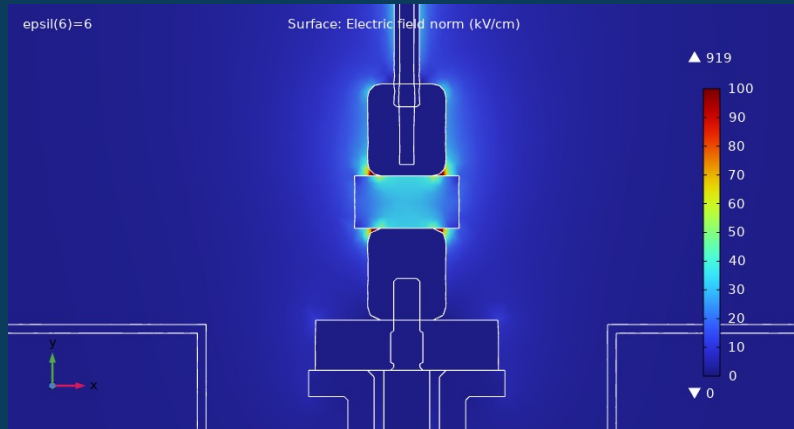
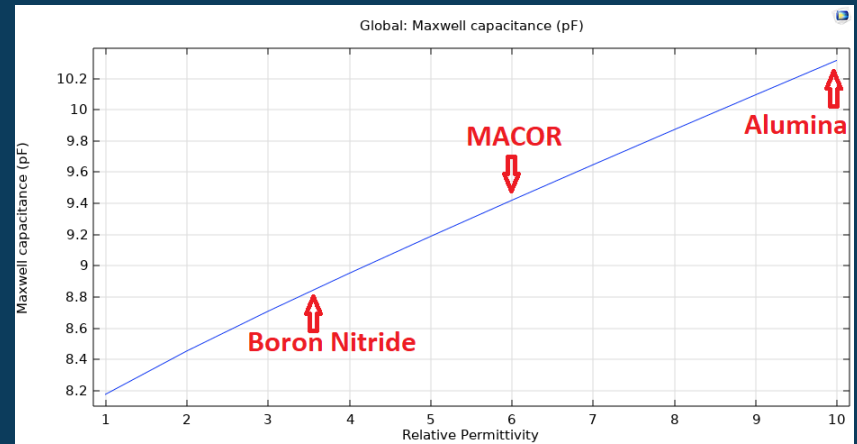
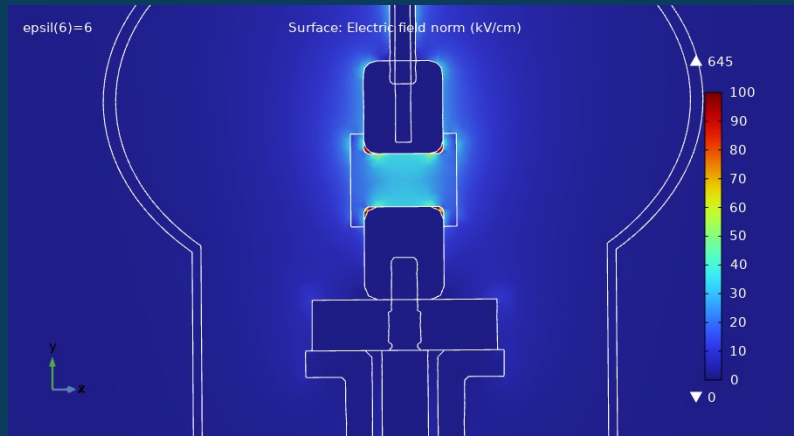
Metal	Cu	Ti	Mo	Mo	Stainless Steel (316)	W	TiAl6V4	Nb	CuCr1Zr	Ta	Ni	Sponge Metal
Grade	OFHC (Grade 101)	Grade 2	99.999%	99.95% (Type 361)	316	99.95%	Grade 5	99.9% pure	-	Tbd	Tbd	Tbd

LONG TERM MILESTONES

Planned
Completed
In Progress







- Resistance = $1.56 T\Omega$ → Leakage current = $25.6 nA$

Seattle, WA Based Lab - ~15,000 sqft

Prototype 1 "Neo"

High Voltage &
Ion Gun

Prototype 2 "Marty"



Material
Sciences
"Janice"

Diagnostics Overview

He3 Neutron counter

- Gives real time neutron flux
- Operates by thermalizing 2.5 MeV neutrons and measuring ionization pulse from He3 thermal neutron capture

Argon Spectroscopy

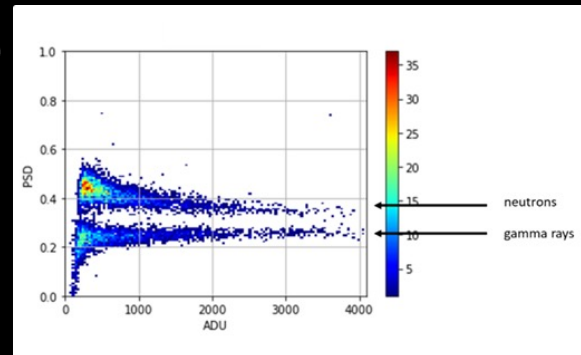
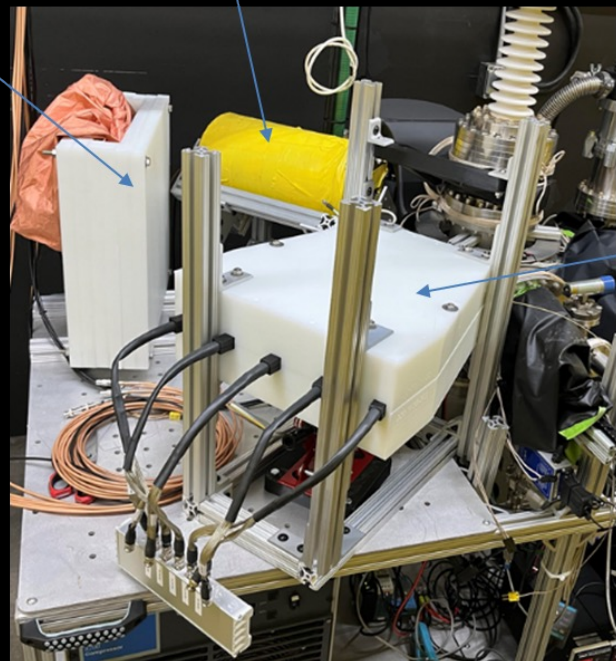
- Fiber optics embedded in anode looking at plasma
- Can measure number of Ar+ ions via measured brightness
- Argon spectroscopy could be alternate method to confirm plasma densification with Ar+ ion and electron confinement in Orbitron

X-ray Spectroscopy

- Measuring Bremsstrahlung X-rays to determine electron energy distribution (Te) and electron density (ne) via X-ray power emitted thru Be window

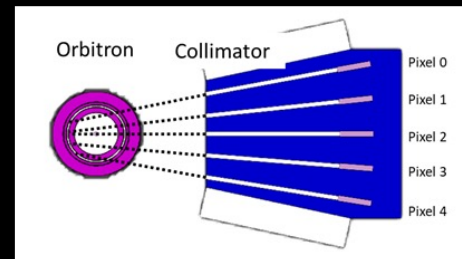
Scintillator w/ Pulse Shape Discrimination (PSD)

- Gives total source neutron flux with high accuracy filtering out gamma rays

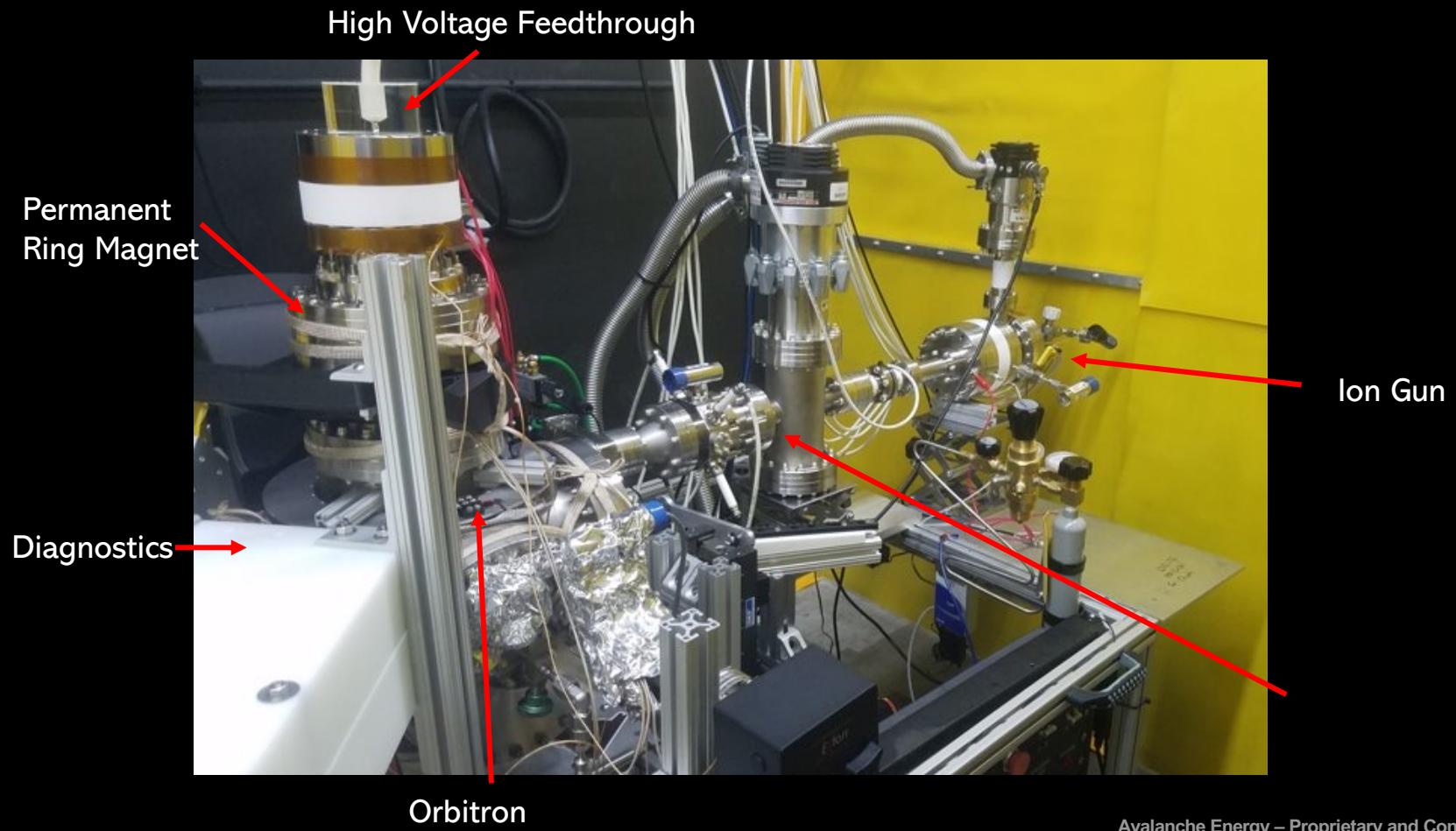


Neutron Camera

- Scintillator w/ PSD collimated view to a "pixel" and locate neutron sources spatially
- Allows discrimination of beam-target fusion in cathode from beam-beam fusion in space between cathode and anode



Prototype 1: "Neo" 100kV, 0.07T

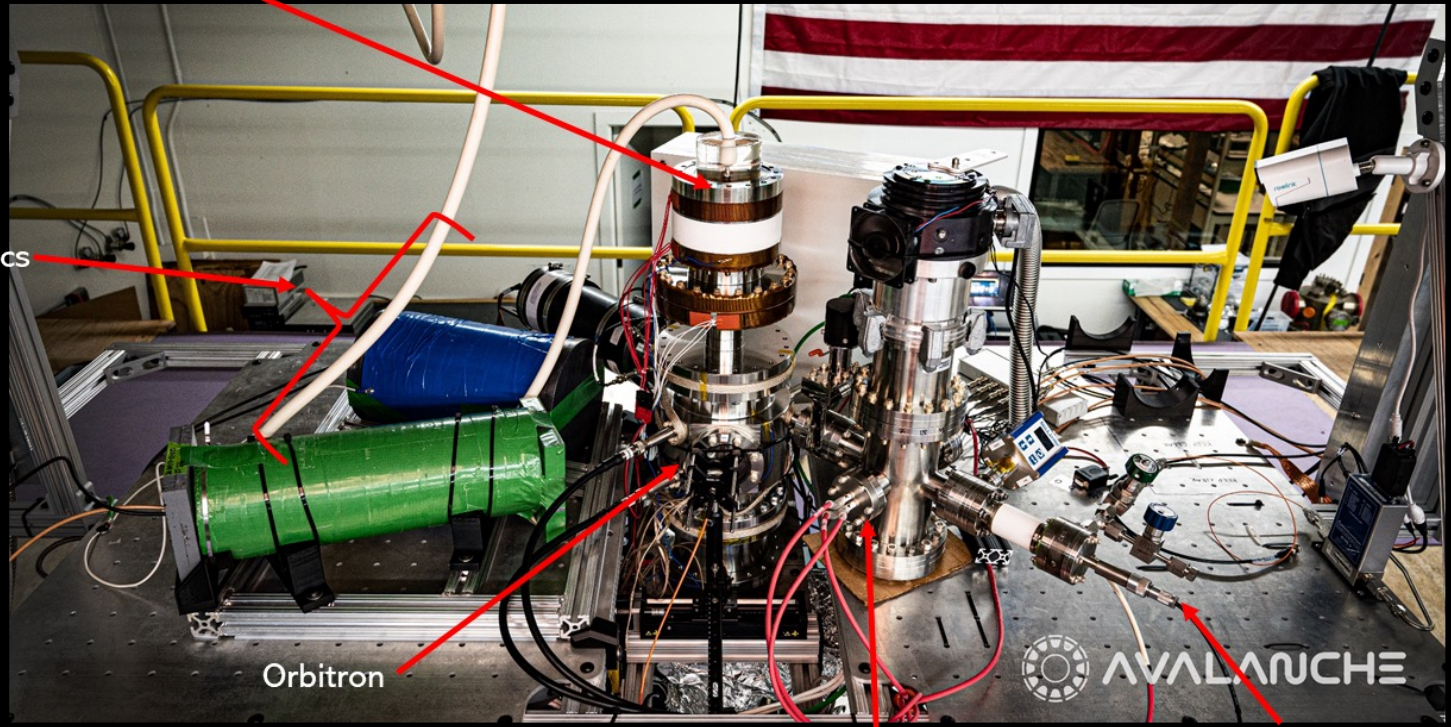


Prototype 2: "Marty" 300kV

High Voltage Feedthrough

Prototype 2 "Marty" – first electrostatic fusion device > 200kV

Diagnostics

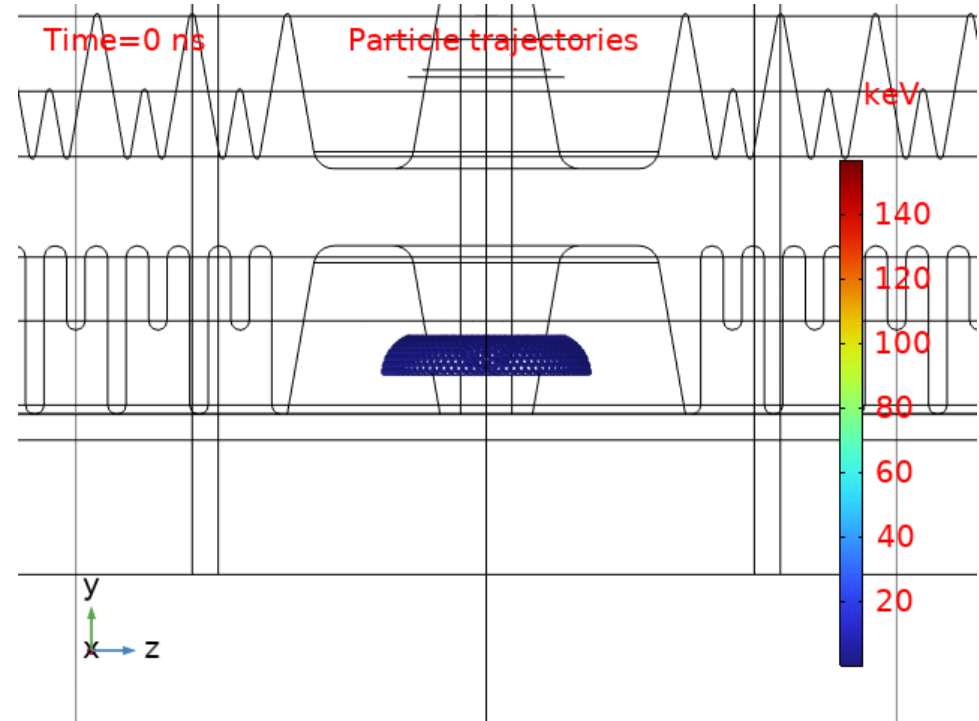


Orbitron

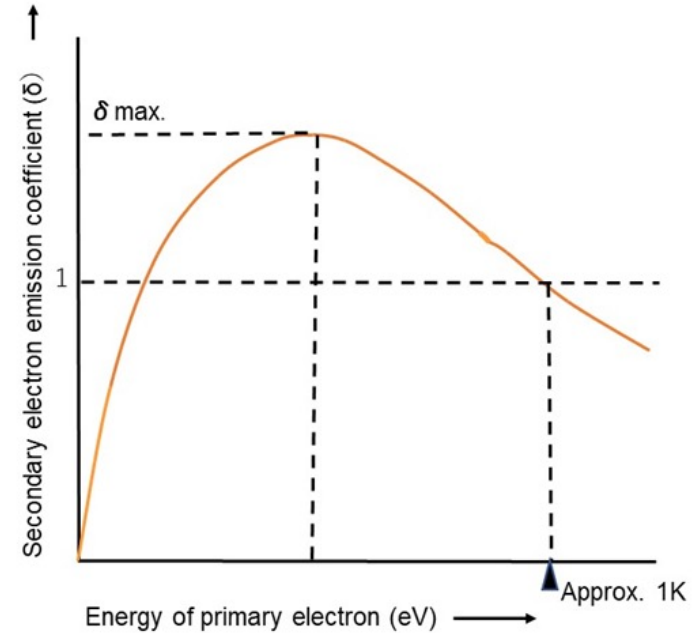


Ion Gun

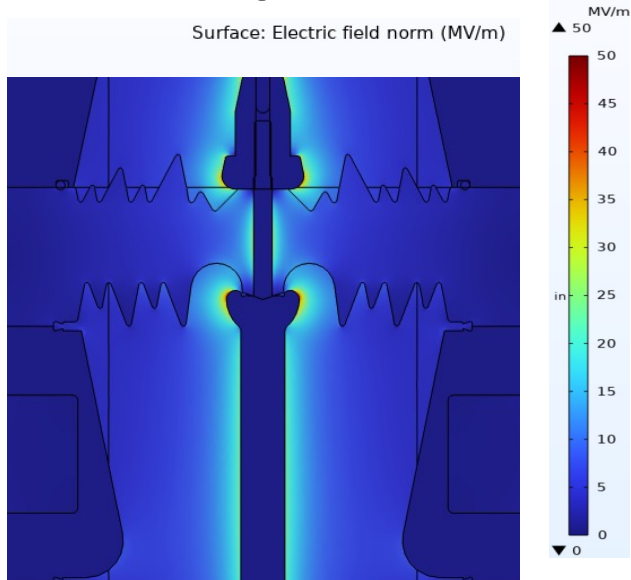
- Particles emit from the cathode part where the field is maximum
- The initial energy of the particles is 1 eV and the initial direction is the same as E-field direction
- In less than 0.1 ns, the particles hit the first ridge with $\sim 150\text{keV}$ energy
- Is that a good number for flashover? Do we prefer a lower energy? Or higher?



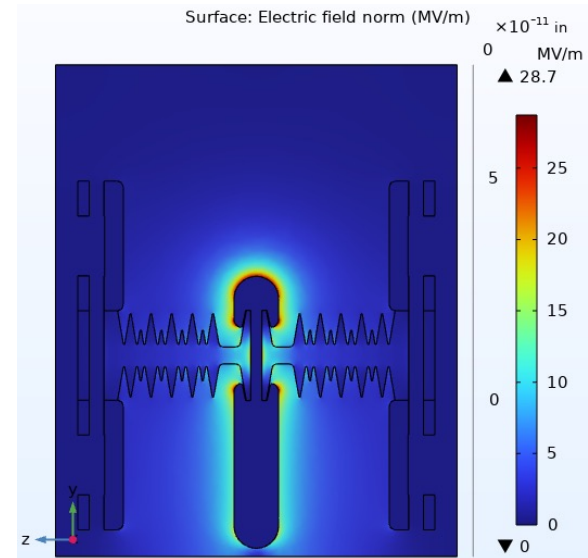
- The secondary electron yield: the number of secondary electrons emitted from a material per incident primary electron.
- At very high energies, the incident primary electrons have a lot of kinetic energy, which means that they penetrate deeper into the material → a decrease in the secondary electron yield.
- At low energies, the incident primary electrons do not penetrate as deeply into the material. Instead, they interact with the outermost layers of atoms, which are more likely to emit secondary electrons.



MAKO V1



MAKO V2

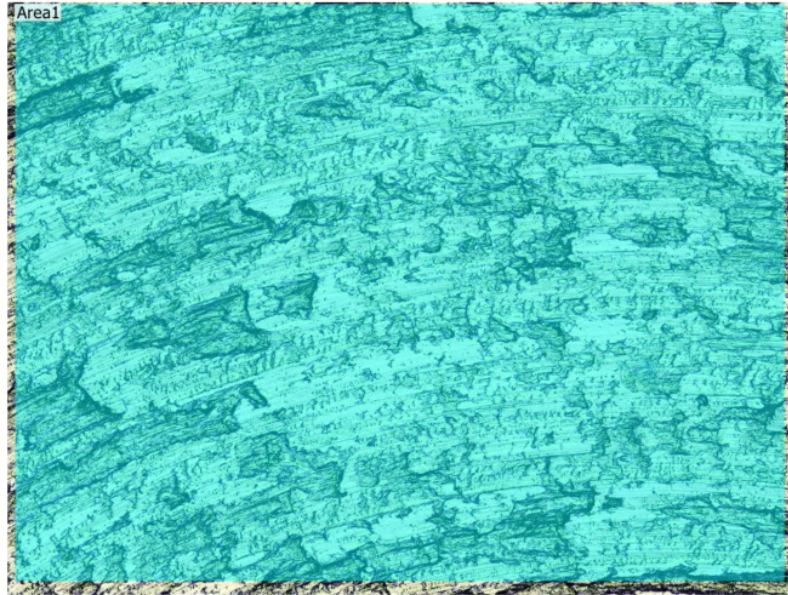


Config.	Electric Field (MV/m)						Flashover Path (mm)
	Cathode TJP	Cathode Corner	Cathode Body (Upper Vac)	Cathode Body (Lower Vac)	AV Insulator	MAX Insulator	
MAKO V1	9-18	46.5	21.9	32.3	3.4	14.9	130
MAKO V2	0.04 (-99%)	32.1 (-31%)	15.0 (-32%)	31.7 (-2%)	2.5 (-27%)	20.0 (+34%)	424 (+326%)
ITER *	0.1	4	-	-	1	-	-
Jim Prop	-	10-20			1-2		

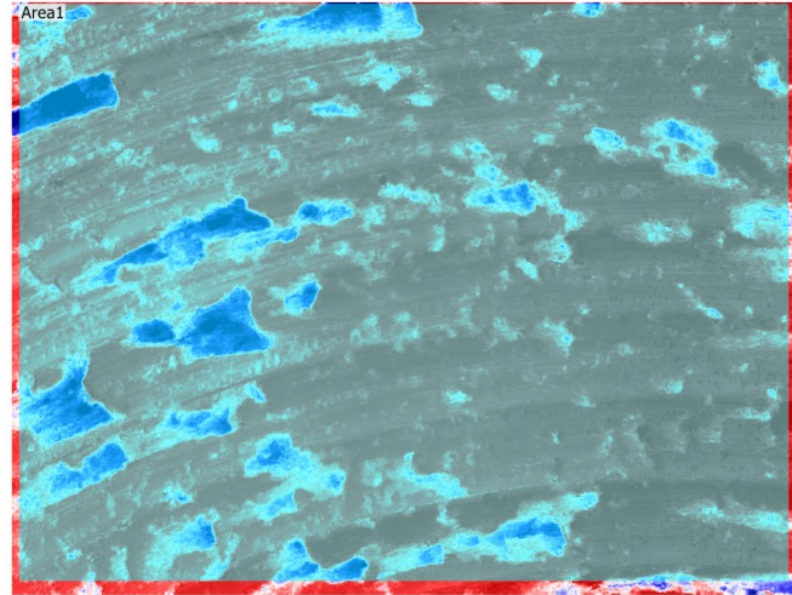
Surface roughness measurement 444 Mo Laser Analysis Input

KEYENCE VK-X3000 Series

Main image



Scale-limited surface

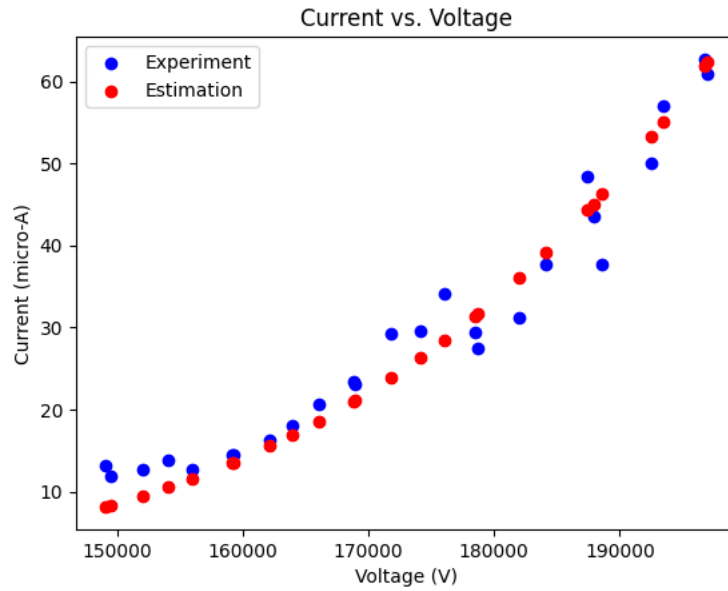


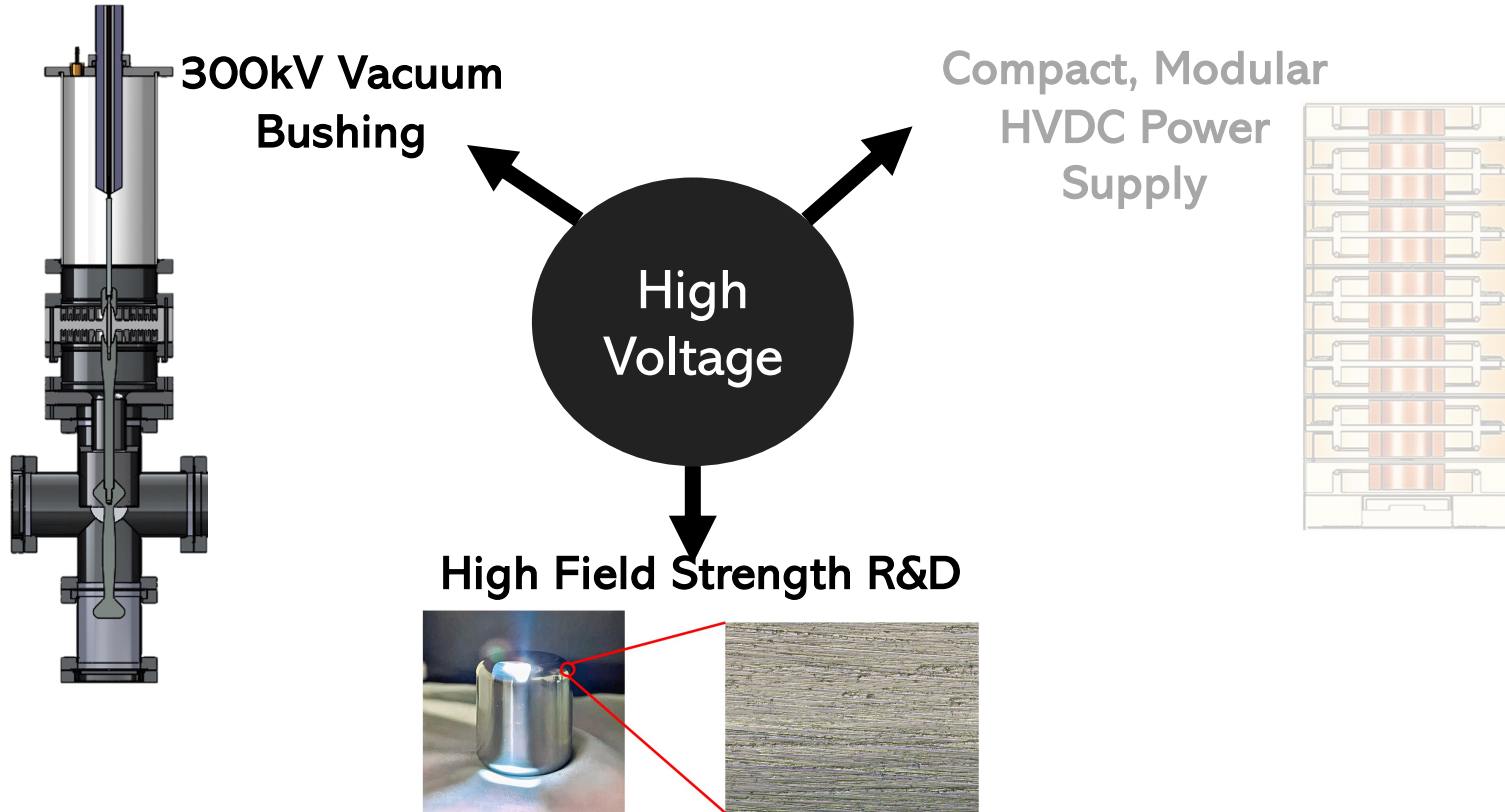
Analysis condition

Roughness standard	ISO 25178-2:2012
Filter type	Gaussian
S-filter	None
F-operation	None
L-filter	None
End effect correction	Enabled

Measurement result

	Sa	Sz	Str	Spc	Sdr
	μm	μm		1/mm	
Max.	0.997	13.856	0.555	1475.171	0.1983
Min.	0.997	13.856	0.555	1475.171	0.1983
Ave.	0.997	13.856	0.555	1475.171	0.1983
Std. DV	0.000	0.000	0.000	0.000	0.000000000

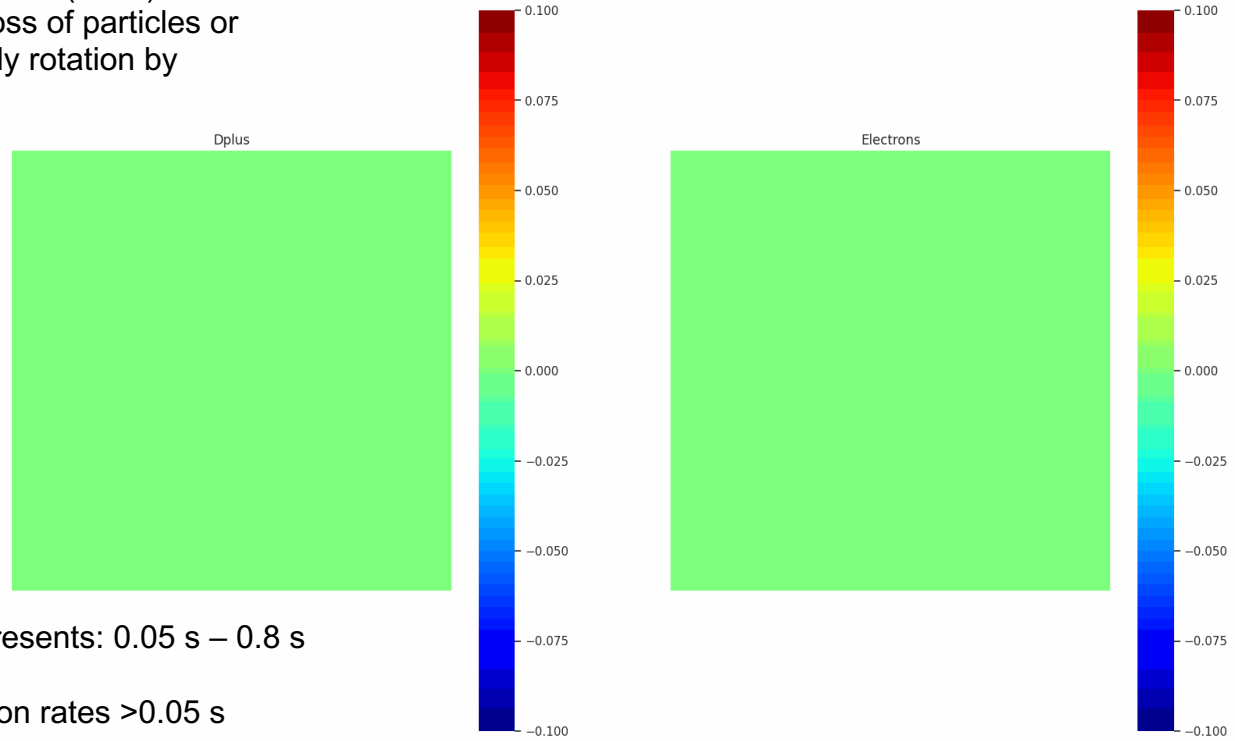




Coulomb Scattering Collisions

Per Rider (1995), Lampe & Manheimer (1998) models should observe complete loss of particles or thermalize to collisionless solid body rotation by 0.05 s

Particle Density at 0.00e+00s | iteration: 0

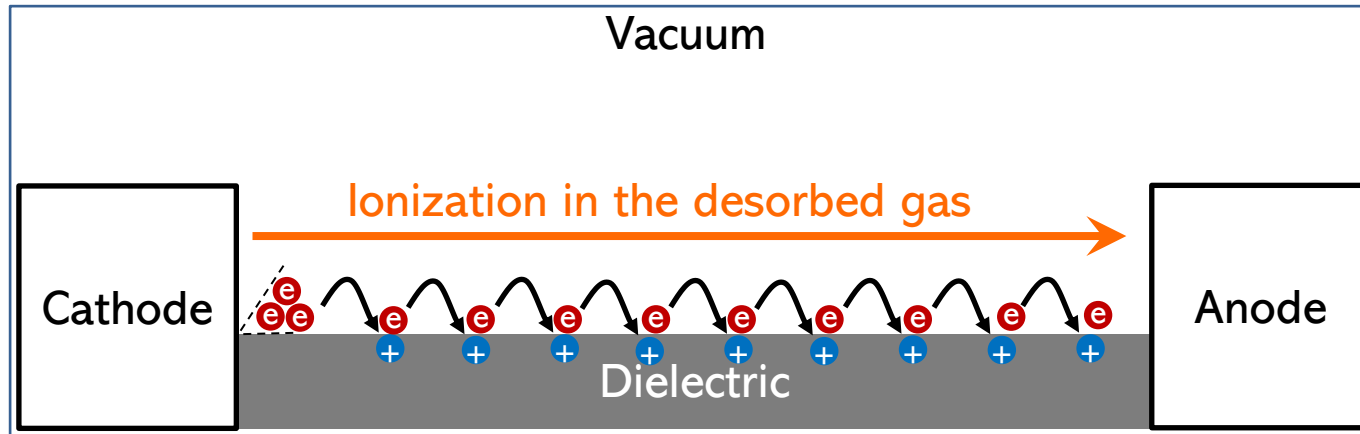


Density scaled simulation time represents: 0.05 s – 0.8 s

Significant particle density and fusion rates >0.05 s

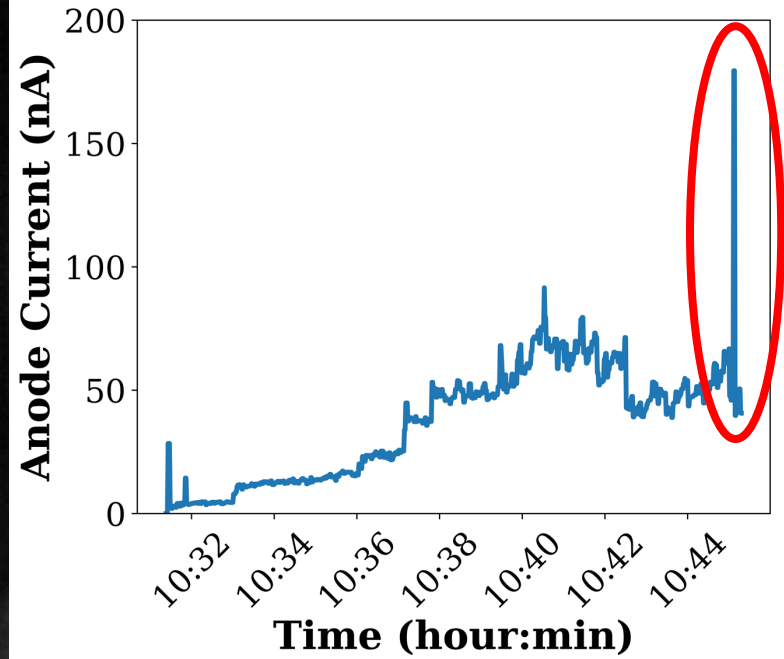
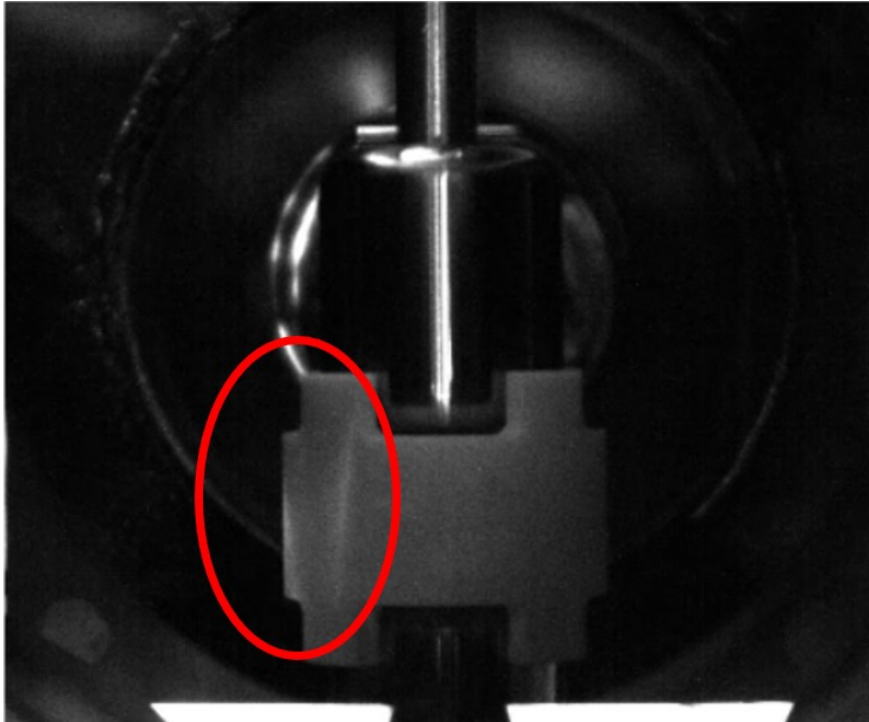
Starting to explore plasma parameter space for beam energy, T_e and Q_{plasma} via these PIC simulations

- (1) field-emission of electrons from the cathode (triple-junction point),
- (2) secondary electron emission avalanche across the surface of the dielectric, and
- (3) Townsend ionization in the desorbed gas from the dielectric's surface



The steps of surface flashover based on SEEA theory

- Capturing surface flashover visually and electrically



- Second Test Campaign: *The Aging Effect of Surface Flashovers*

